Sedimentology of alpine debris-flow and talus deposits in Sacajawea cirque Bridger Range, Montana
by Amanda Vrooman Werner

A thesis submitted in partial fulfillment of the requirements for the degree of Master of Science in Earth Sciences
Montana State University

Abstract:
Well-formed deposits of modern debris flows and talus were studied in Sacajawea cirque, located in the Bridger Range of southwestern Montana. Debris flows possess a wide range of sedimentologic characteristics, particularly fabrics and sedimentary structures. These characteristics were examined in the deposits in order to develop criteria to aid in the recognition of debris-flow deposits in the rock record. As debris flows and talus often share similar fabrics and textures, these characteristics were examined in both types of deposits to determine if there were differences which could then be applied to differentiation of similar types of deposits in the rock record.

Study of debris-flow fabrics reveals clast-supported rather than the more common matrix-supported fabric. This suggests that clast-supported fabric should also be recognized as a common debris flow characteristic. Quantitative analysis of clast fabric by the eigenvalue method shows that clasts in levees have a weak downstream orientation and also dip downstream, while lobes show no preferred orientation of clasts.

Textural analysis of the debris-flow deposits shows that clasts larger than 64 mm are cobble- to boulder-size and subrounded. Forty percent of clasts larger than 64 mm come from the Lodgepole limestone, or the source of the talus, suggesting that the talus contributes clasts to the debris flow source area. The large percentage of silt (54%) and clay (10%) in the matrix shows that less resistant rock units in the source area (Three Forks and Sappington shale and siltstone and basal shale from the Lodgepole) contribute to the finer matrix because these units are less resistant to weathering. The bulk of the deposit is massive while the top is coarse-tail inversely graded.

Fabric analysis of the talus reveals a clast-supported framework and clasts alligned weakly parallel to the slope direction and dipping downslope at steep angles. Textural analysis reveals the talus deposits consist of angular, cobble- to boulder-size clasts of Lodgepole limestone.

Overall, the debris flow and talus deposits are similar sedimentologically because talus deposits contribute clasts to the debris flow source area. Thus, sedimentologists should use caution in identification of both types of deposits in the rock record.

SEDIMENTOLOGY OF ALPINE DEBRIS-FLOW AND TALUS DEPOSITS IN SACAJAWEA CIRQUE BRIDGER RANGE, MONTANA

by

Amanda Vrooman Werner

A thesis submitted in partial fulfillment
of the requirements for the degree

of

Master of Science

in

Earth Sciences

MONTANA STATE UNIVERSITY
Bozeman, Montana

May, 1994

APPROVAL

of a thesis submitted by

Amanda Vrooman Werner

This thesis has been read by each member of the thesis committee and has been found to be satisfactory regarding content, English usage, format, citations, bibliographic style, and consistency, and is ready for submission to the College of Graduate Studies.

5/22/94 — Date

James Schmidt — Chairperson, Graduate Committee

Approved for the Major Department

5-25-94 — Date

Head, Major Department

Approved for the College of Graduate Studies

6/9/94 — Date

Graduate Dean

STATEMENT OF PERMISSION TO USE

In presenting this thesis in partial fulfillment of the requirements for a master's degree at Montana State University, I agree that the Library shall make it available to borrowers under rules of the Library.

If I have indicated my intention to copyright this thesis by including a copyright notice page, copying is allowable only for scholarly purposes, consistent with "fair use" as prescribed in the U.S. Copyright Law. Requests for permission for extended quotation from or reproduction of this thesis in whole or parts may by granted only by the copyright holder.

Signature Amanda Kaaman Werner

Date 5-25-94

ACKNOWLEDGEMENTS

I would like to thank my husband, Jordan, for both emotional and financial support. Thanks also go to Joe Stock and Jeralyn Brodowy for their help in the field and to Mark Cechovic and Paul Azevedo for advice on various aspects of my research. I also thank Jim Schmitt for his advisement on this project and Steve Custer and Bill Locke for their contributions as my committee members.

I am very grateful for financial assistance provided by the Montana State University Earth Science Department Graduate Research Teaching Assistantship, Donald L. Smith Memorial Scholarship and the Yellowstone Center for Mountain Environments.

TABLE OF CONTENTS

TABLE OF CONTENTS-Continued

LIST OF TABLES

LIST OF FIGURES

LIST OF FIGURES-Continued

LIST OF PLATES

[Plates in back pocket]

GLOSSARY

Eigenvalue Terminology

A_{0-90}, A_{0-180} Values representing the mean absolute differences between the orientation of V_1 and the local flow direction. A_{0-90} shows whether clast long-axes are aligned parallel to flow (values near 0 degrees) or transverse to flow (values near 180 degrees). A_{0-180} shows if parallel clasts dip upflow (values near 180 degrees) or downflow (values near 0 degrees).

D_1 The mean dip of V_1.

D_3 The mean dip of V_3.

S_1 A normalized eigenvalue which indicates the mean strength of V_1. A larger S_1 value indicates strong fabric.

S_3 A normalized eigenvalue which represents the mean strength of V_3.

V_1 An eigenvector representing the axis of maximum concentration of the clast long-axes.

V_3 An eigenvector which represents the axis of minimum concentration of the clast long-axes. It is perpendicular to V_1.

ABSTRACT

Well-formed deposits of modern debris flows and talus were studied in Sacajawea cirque, located in the Bridger Range of southwestern Montana. Debris flows possess a wide range of sedimentologic characteristics, particularly fabrics and sedimentary structures. These characteristics were examined in the deposits in order to develop criteria to aid in the recognition of debris-flow deposits in the rock record. As debris flows and talus often share similar fabrics and textures, these characteristics were examined in both types of deposits to determine if there were differences which could then be applied to differentiation of similar types of deposits in the rock record.

Study of debris-flow fabrics reveals clast-supported rather than the more common matrix-supported fabric. This suggests that clast-supported fabric should also be recognized as a common debris flow characteristic. Quantitative analysis of clast fabric by the eigenvalue method shows that clasts in levees have a weak downstream orientation and also dip downstream, while lobes show no preferred orientation of clasts.

Textural analysis of the debris-flow deposits shows that clasts larger than 64 mm are cobble- to boulder-size and subrounded. Forty percent of clasts larger than 64 mm come from the Lodgepole limestone, or the source of the talus, suggesting that the talus contributes clasts to the debris flow source area. The large percentage of silt (54%) and clay (10%) in the matrix shows that less resistant rock units in the source area (Three Forks and Sappington shale and siltstone and basal shale from the Lodgepole) contribute to the finer matrix because these units are less resistant to weathering. The bulk of the deposit is massive while the top is coarse-tail inversely graded.

Fabric analysis of the talus reveals a clast-supported framework and clasts alligned weakly parallel to the slope direction and dipping downslope at steep angles. Textural analysis reveals the talus deposits consist of angular, cobble- to boulder-size clasts of Lodgepole limestone.

Overall, the debris flow and talus deposits are similar sedimentologically because talus deposits contribute clasts to the debris flow source area. Thus, sedimentologists should use caution in identification of both types of deposits in the rock record.

INTRODUCTION

Importance of Study

Debris-flow deposits exhibit complex and variable sedimentologic characteristics, particularly fabrics and sedimentary structures (Smith, 1986). Matrix-supported fabric is cited as a common characteristic of debris flows (Smith, 1986; Costa, 1988; Eyles and Kocsis, 1988; Hubert and Filipov, 1989). However, clast-supported debris-flow deposits have also been recognized (Rodine and Johnson, 1976; Lowe, 1982; Costa, 1984; Shultz, 1984). Orientations of the long-axis of clasts are typically described as parallel to the flow direction (Johnson and Rodine, 1984; Smith, 1986; Eyles and Kocsis, 1988); however, random orientations have also been reported (Lawson, 1979a; Hubert and Filipov, 1989). Sedimentary structures such as weak inverse and normal grading have been documented by Eyles and Kocsis (1988), whereas Smith (1986) and Costa (1988) noted that sedimentary structures, including stratification, are absent in debris-flow deposits. This variability in sedimentologic characteristics may cause difficulty in recognizing ancient deposits (Eyles et al., 1988). Further study is desirable to explore the range of fabrics and

sedimentary structures which characterize modern debris-flow deposits.

Debris-flow deposits share similar fabrics and structures with other types of flow deposits, such as hyperconcentrated flows and stream flows. This similarity may cause difficulty in distinguishing one type of deposit from another (Smith, 1986; Costa, 1988). The establishment of more precise sedimentologic criteria for recognition of debris-flow deposits will enhance sedimentologic differentiation of different types of flow deposits. This knowledge of sedimentologic features may then be applied to the recognition and interpretation of similar debris-flow deposits in the rock record.

Debris-flow deposits appear similar to talus deposits in the rock record. Both are coarse-grained and poorly sorted. As a result, few ancient talus deposits have been recognized (Tanner and Hubert, 1991). The sedimentologic characteristics of both modern debris-flow and talus deposits may be similar because talus often contributes the material for debris flows (Fryxell and Horberg, 1943). By studying clast fabric and grain size of both modern debris-flow and talus deposits, sedimentary criteria may be developed to aid in the differentiation and recognition of these types of deposits in the rock record.

Sacajawea cirque, located in the Bridger Range of southwestern Montana, contains excellent exposures of both

modern debris-flow and talus deposits. The morphologies of debris flows, such as levees and lobes, are well preserved and exposed, as are talus slopes. Documentation of fabrics and structures in well developed debris-flow and talus deposits allows comparison. Thus, Sacajawea cirque is a ideal site for studying the geomorphic and sedimentologic characteristics of both debris-flow and talus deposits.

Questions

The questions answered in this thesis are: (1) What are the geomorphic characteristics and sedimentary fabrics, textures, and structures of the debris-flow deposits in Sacajawea cirque? (2) What are the sedimentary fabrics and textures of the talus deposits in Sacajawea cirque? (3) Do the deposits of debris flows and talus slopes in Sacajawea cirque differ sedimentologically? If so, what sedimentologic criteria distinguish one deposit from another?

STUDY AREA

Location of Study Site

Sacajawea cirque is in the Bridger Range of southwestern Montana (Figure 1). The range is a small (40 km long), north-trending uplift of Archean and Proterozoic basement rocks overlain by steeply east-dipping Paleozoic through Mesozoic sedimentary rocks (Lageson, 1989). The steeply dipping strata (approximately 65 degrees) are the east limb of an asymmetric, north-plunging anticline that formed during the late Paleocene to early Eocene and was truncated by a north-trending, down-to-the-west normal fault (Lageson, 1989). Nowhere are those strata better exposed than in the walls of Pleistocene cirques, carved out on the eastern side of the range (Locke and Lageson, 1989). The largest, most well-developed cirque in the range is referred to as Sacajawea cirque. This cirque is just north of Sacajawea Peak, the highest peak in the range (elevation 2947 m).

The floor of Sacajawea cirque lies at an elevation of 2560 meters and is surrounded by steep rock walls that rise 180 meters above the floor. The cirque walls contain strata that are younger at the mouth of the cirque and older at the

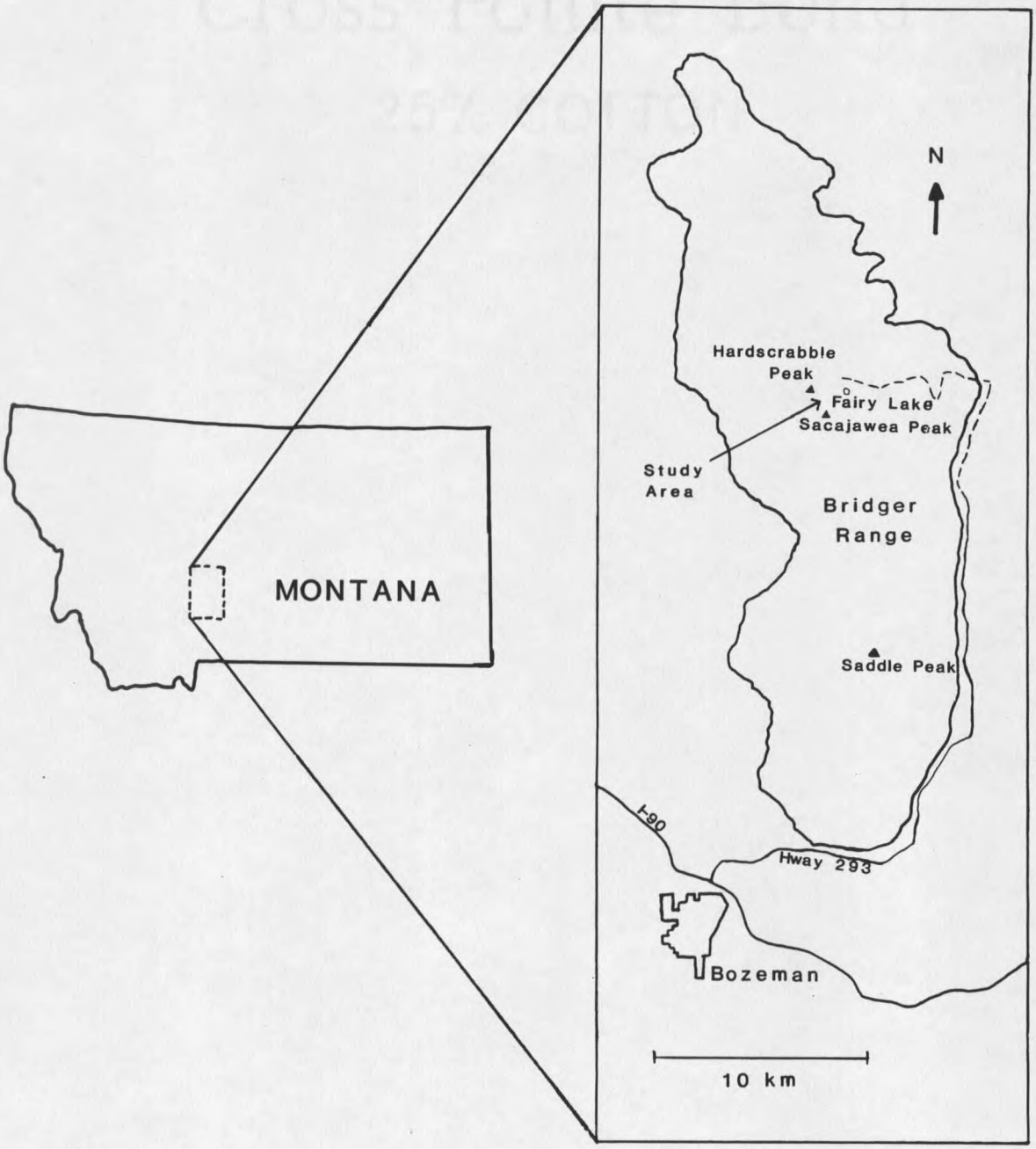

Figure 1. Location of Sacajawea cirque, Bridger Range, Montana. Dashed lines indicate unpaved road.

headwall. The various rock units are described in detail in a diagrammatic stratigraphic column (Figure 2). A brief description of the units follows. Beginning with the oldest unit present in the cirque, the Cambrian Pilgrim Formation consists of limestone-pebble conglomerate interbedded with green shale and bounded on the top and bottom by oolitic limestone. The Cambrian Snowy Range Formation consists of two members. The Dry Creek Shale member contains gray-green shale interbedded with calcareous siltstone and sandstone. The Sage Pebble member contains dense limestone and limestone pebble conglomerate. The Devonian Maywood Formation consists of thin-bedded calcareous siltstone. The Devonian Jefferson Formation contains dolomite and limestone interbedded with dolomitic siltstone. The Devonian Three Forks Formation contains thin-bedded silty limestone that overlies brecciated limestone and a basal layer of limonite nodule shale and siltstone. The Devonian Sappington Formation is composed of fine-grained calcareous siltstone and sandstone bounded on the top and bottom by shale. The Mississippian Lodgepole Formation consists of thin- to medium-bedded fossiliferous limestone overlying black shale. The Mission Canyon Formation consists of massive limestone (McMannis, 1955). These rock units contribute to the landforms found on the floor of the cirque including rock glaciers, protalus ramparts, talus slopes, and debris-flow deposits (Locke and Lageson, 1989) (Figure 3).

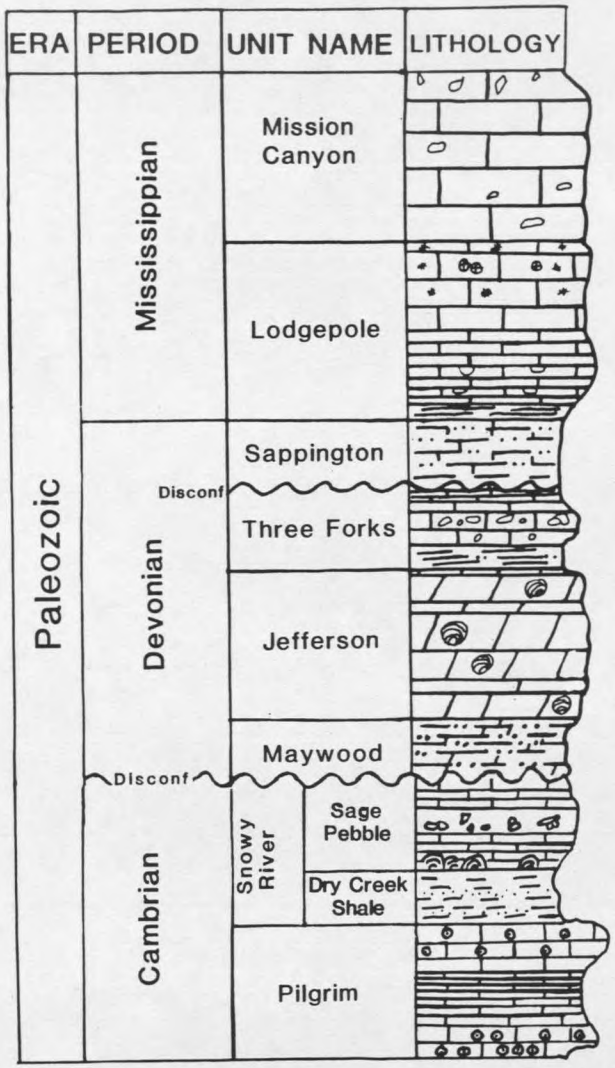

Description

Light gray, massive or poorly bedded, resistant limestone with solution breccias. Contains chert nodules. (430-905')

Dark gray medium-bedded fossiliferous limestone. Lower dark gray, thin-bedded limestone with chert nodules. Black shale at base. (600-810')

Buff-brown, thin- to medium-bedded, fine-grained calcareous siltstone and sandstone. Basal, black shale. (46-100')
Upper gray, thin-bedded silty limestone. Middle buff, medium-bedded brecciated limestone. Basal, limonite-nodule shale, and siltstone. (100-150')

Brown, thick-bedded dolomite and limestone, containing stromatoporids. Intercalated yellow-pale pink dolomitic siltstone beds. (400-620')

Yellow to brown, thin-bedded calcareous siltstone with some dolomite. (39-92')
Fine-grained, thin-bedded, dense limestone and limestone pebble conglomerate. (121-204')
Gray-green shale with interbedded yellow calcareous siltstone and sandstone. (50-76')
Dark gray, medium-bedded, oolitic limestone. Middle, gray to yellow-brown thin-bedded limestone with limestone-pebble conglomerate and inter-bedded green shale.
Gray, massive oolitic, limestone. (363-433')

Figure 2. Diagrammatic stratigraphic column of rock units present in Sacajawea cirque (After McMannis, 1955).

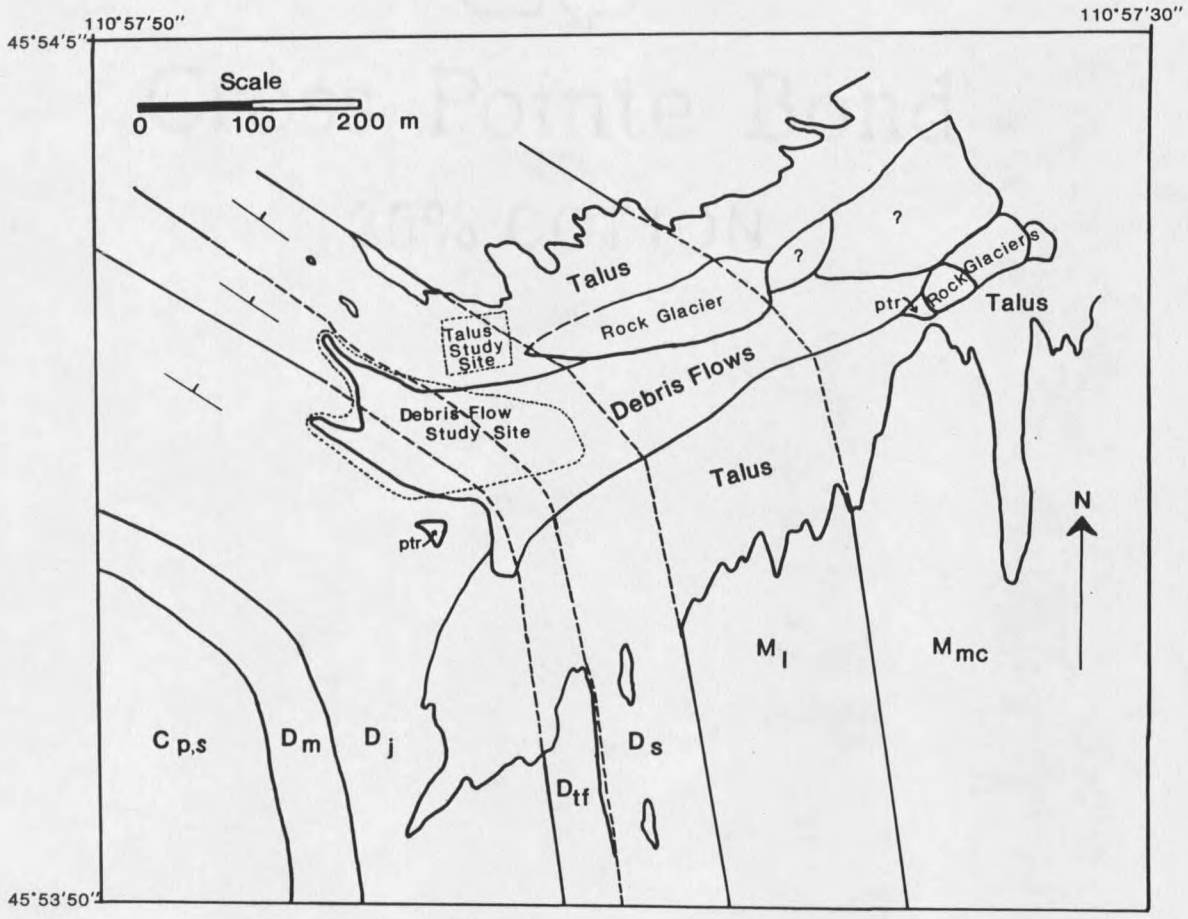

Figure 3. Geology and geomorphic landforms of Sacajawea cirque. Study sites for both debris flows and talus are delineated. The symbol "ptr" indicates protalus rampart. Areas marked with an "?" are unidentified landforms mapped by Locke and Lageson (1989). Rock units are Mississippian Mission Canyon (Mmc) and Lodgepole (Ml) limestone and dolomite; Devonian Sappington (Ds) shale and calcareous siltstone; Three Forks (Dtf) silty and brecciated limestone; Jefferson (Dj) limestone, and Cambrian Pilgrim limestone and Snowy River shale and limestone pebble conglomerate (Cp,s). Strike and dip symbols show the structural orientation of the bedrock (After Locke and Lageson, 1989).

The vegetation in the cirque reflects the alpine environment. Krummholz, or deformed dwarfed shrub trees, occur on the windswept floor of the cirque (Ross and Hunter, 1976). Cushion plants such as moss campion and grasses such as alpine bluegrass and sheep fescue are found on and among rocks (Ross and Hunter, 1976).

The floor of Sacajawea cirque is covered with modern debris-flow deposits, including levees and lobes. These debris-flow deposits have been dated by lichenometry and tree-ring analysis and range in age from less than 25 to 300-years old (Locke and Lageson, 1989). At the mouth of the cirque, debris-flow deposits are partially covered with soil and vegetation and difficult to recognize. However, below the headwall of the cirque, six debris-flow channels outlined by levees and lobes can be differentiated. These deposits were chosen for study because their well-developed lobes and levees provide good exposures for mapping of geomorphic features and study of sedimentologic characteristics.

Description of Study Site

The Sacajawea cirque debris-flow deposits are on a debris-flow fan. Debris-flow fans have an area less than 2 km^2, a slope ranging from 5 to 20 degrees, and are composed of debris-flow deposits (Ono, 1990; Kochel, 1990; Whipple and Dunne, 1992). The debris-flow fan in Sacajawea cirque

has an area of 0.03 km^2 and a slope ranging from 9 to 24 degrees. The fan surface is covered with overlapping debris-flow deposits as evidenced by the well-developed levees and lobes (Figure 4).

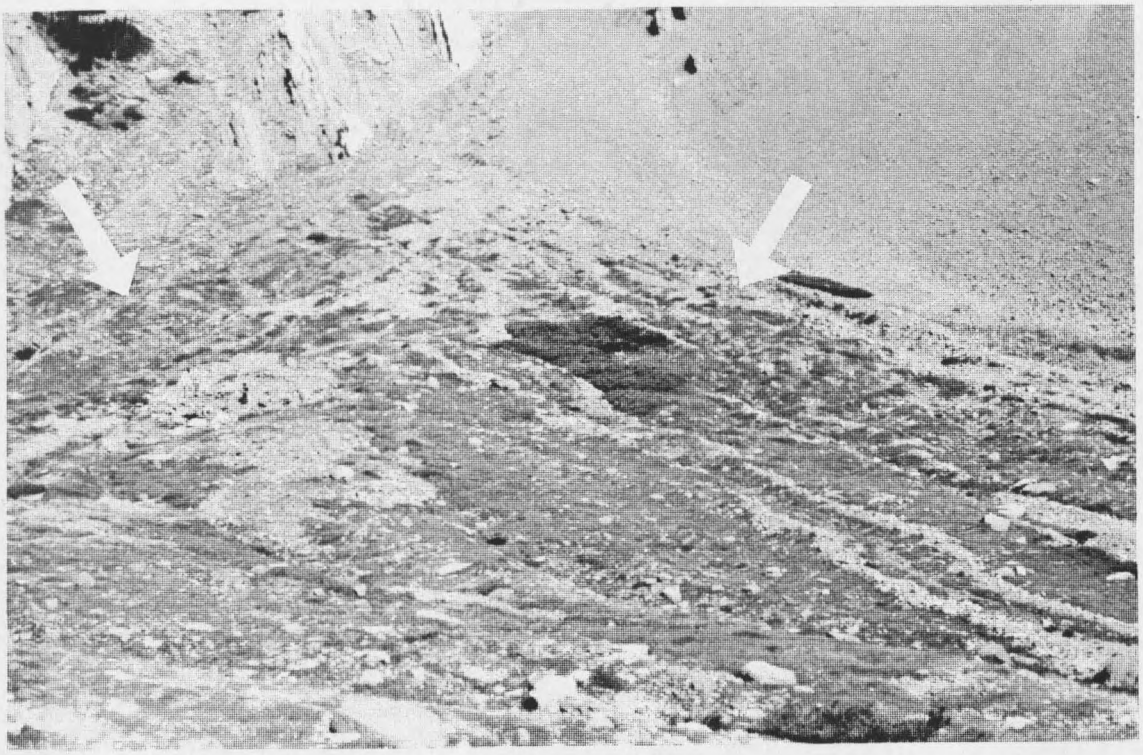

Figure 4. Debris-flow fan in Sacajawea cirque located between arrows. Talus slopes are visible in the upper right corner.

The fan extends from a small, steep drainage or gully on the northwest side of the cirque. The gully extends to the top of the cirque wall along the Three Forks Formation, and is filled with a variety of clast sizes derived from the surrounding bedrock exposures and talus slopes.

The fan consists of a variety of debris-flow morphologies which will be described in greater detail

later. The apex of the fan consists of abundant overlapping debris-flow deposits. In the mid-fan area, the fan is incised by channels which extend the entire length of the fan and are bordered by bouldery levees and scattered lateral lobes. In-channel lobes block some reaches of the channels. At the distal part of the fan, thin terminal lobes spread out from the mouths of the channels.

Talus slopes are found on the northwest and southeast walls of the cirque. The talus slopes chosen for study are located on the north side of the fan, in some areas overlap the gully, and extend from the Lodgepole and Mission Canyon Formations. Figure 4 and Plate 1 show the talus slopes.

TERMINOLOGY

Debris Flows

Debris flows are gravity-induced mass-movements of granular solids with minor amounts of clay, entrained in water and air (Costa, 1984). The flows leave deposits that are very poorly sorted, lack internal stratification, and support the largest clasts in a finer-grained matrix (Smith, 1986). Debris flows occur in mountainous areas in all climates. Conditions required for debris flow initiation include: an abundant source of unconsolidated fine-grained rock and soil debris, steep slopes, sparse vegetation, and a large but intermittent source of moisture (Costa, 1984). Other terms which have been used to identify the same or closely related processes are debris slide, mudflow, mud slide, earth flow, mudspate, tillflow, and lahar (Johnson and Rodine, 1984).

Debris flows are some of the most threatening natural phenomena in the world. Each year, debris flows claim hundreds of lives and cause millions of dollars of property damage worldwide (Costa, 1984). In Japan alone, an average of 90 lives are lost annually from debris flows (Takahashi, 1981). In 1919, a volcanic ejection of water from a crater lake created massive debris flows that killed 5100 people,

destroyed 140 villages, and buried 130 km^2 of land in Java (Johnson and Rodine, 1984). This worldwide destruction by debris flows has led to their study in Japan, Brazil, New Zealand, California, Utah, Alaska, Idaho, Arizona, Pennsylvania, and Virginia (Costa, 1984; Johnson and Rodine, 1984). Debris flows have been most widely studied in the American southwest (Johnson and Rodine, 1984). Alpine debris flows have been studied to a lesser extent in Canada (Owens, 1973), the Yukon (Broscoe and Thomson, 1969), Colorado (Curry, 1966), Wyoming (Fryxell and Horberg, 1943), and Scandinavia (Rapp and Nyberg, 1981).

Morphologic Characteristics

Debris flows form distinctive landforms. The flows form their own channels as particles pushed to the side form linear ridges or levees (Sharp, 1942). The flow front moves forward in successive waves or surges. These surges may be deposited in the middle of the channel as medial deposits or in-channel lobes (Johnson and Rodine, 1984). When the debris flow stops, the front of the flow leaves a terminal lobe with a steep front and sides (Costa, 1984). Debris flows may be blocked by in-channel lobes, diverted out of the channel, and deposited as lateral lobate projections or lateral lobes (Sharp, 1942).

Rheologic and Sedimentologic Characteristics

Debris flows, hyperconcentrated flows, and stream flows can be distinguished based upon rheologic or flow deformation characteristics (Table 1). Debris flows have 70-90% sediment by weight, and the sediment and water move together as a viscoplastic body. Flow type is laminar and the dominant particle support mechanisms are cohesive matrix strength, buoyancy, and dispersive pressure. In contrast, stream flows are dilute, having 1-40% sediment by weight with the sediment and water acting as two separate phases. As stream flows are turbulent, turbulence serves as a sediment support mechanism along with electrostatic charges on small particles. Hyperconcentrated flows are intermediate in nature, having 40-70% sediment by weight, and are partially turbulent and partially laminar. Particle support mechanisms are buoyancy and dispersive stress.

Though each of these flow types possess distinct rheologic characteristics, their sedimentologic characteristics may overlap (Table 1), and make distinction between flow types difficult. For example, debris-flow deposits may be ungraded, inversely graded, inversely-to-normally graded, or rarely coarse-tail normal graded throughout the unit (Smith, 1986). Hyperconcentrated flows and stream flows may also exhibit normal and inversely graded deposits. Matrix-supported fabric is cited as

Table 1. Rheologic and sedimentologic characteristics of debris Flows, hyperconcentrated flows, and stream flows (After Smith, 1986; Costa, 1988).

Characteristics	Debris Flows	Hyperconcentrated Flows	Stream Flows
Sediment Concentration	70-90% by weight	40-70% by weight	1-40% by weight
Shear Strength	present, high	present, but small	absent
Flow Type	laminar	turbulent to laminar	turbulent
Major Sediment Support Mechanisms	cohesion, buoyancy, dispersive stress	buoyancy, dispersive stress	turbulence, electrostatic charges,
Mode of Deposition	en masse	grain-by-grain, suspension and traction	grain-by-grain, traction-dominated
Stratification	none	none or horizontal stratification	massive or horizontal stratification
Grading	none; inverse; inverse to normal; coarse-tail normal	normal or inverse	variable
Clast Packing	matrix-supported; rarely clast-supported	clast-supported	clast-supported
Clast long-axis orientation; imbrication	parallel or transverse; parallel most common; poor imbrication	transverse to flow; poor imbrication	transverse to flow; well imbricated

diagnostic of debris-flow deposits by many workers (Smith, 1986; Costa, 1988; Eyles and Kocsis, 1988; Hubert and Filipov, 1989); however, some workers have recognized clast-supported debris-flow deposits (Curry, 1966; Rodine and Johnson, 1976; Lowe, 1982; Shultz, 1984; Blair, 1987). These clast-supported debris-flow deposits may look similar to clast-supported hyperconcentrated-flow or stream-flow deposits.

Talus

Talus is an accumulation of rock debris of various sizes transported from a mountain valley wall by gravity, runoff from rain or snow, or by avalanching snow to a valley floor below (White, 1981). Modern talus accumulations typically have slopes of 32 to 40 degrees with a concave-up profile. The largest clasts are found at the base of the slope, while the smaller ones are present higher on the slope (Rapp and Fairbridge, 1968). Talus deposits are poorly sorted, clast-supported, angular, and particle sizes are positively skewed towards the larger clasts. Clast fabric is most often parallel to the depositional surface, with plate-shaped clasts dipping at approximately 34 degrees, often upslope (Rapp and Fairbridge, 1968). Talus is often found in association with debris flows, as it may contribute to or be the source of debris-flow deposits (Fryxell and Horberg, 1943).

METHODS

Geomorphic Characteristics

In order to study the morphologic characteristics of the channels and debris-flow deposits, the location of channels and spatial distribution of different types of deposits were mapped on oblique photos of the fan. Each part of the deposit was described and photographed. Measurements of channel length, width, and depth were made to characterize the sizes of channels present on the fan. The gradients of the deepest channels were measured with a hand level and tape measure every 5 meters in order to show the step-like character of the channels.

Sedimentologic Characteristics

Fabric

The fabric of the debris-flow deposits was documented by studying both clast packing and clast orientation on the surface of the deposits. Clast packing was described as either matrix-supported (the largest clasts are suspended in a finer matrix of silt and clay-size particles) or clast-supported (the largest clasts touch each other and there is

little finer matrix). Matrix was defined as particles <4 mm (Major and Voight, 1986). Clast packing was observed in vertical sections.

Clast orientation was documented in levees and lobes for clasts >64 mm. Grids were set up at 20 meter intervals down the most continuous levees. Twenty-six sample sites were examined on levees and lobes so as to represent each part of the deposit (Plates 1 and 2). The trend and plunge of the long axis was measured for elongate and bladed clasts. Elongate clasts are defined as those with a/b/c ratios of a/b>2 and b=c. Bladed clasts are those with a/b/c>3/2/1 (a, b, and c are the long, intermediate, and short axes, respectively). Imbricated elongate/bladed clasts were noted. The strike and dip of the ab-plane was measured for imbricated platy clasts (those with a=b and a/c>2). At each sample site, at least 15 clasts were measured. Also measured at each site was the downstream flow direction of the levee or lobe.

Using the program Spheristat by Frontenac Wordsmith, Inc., the trend and plunge of elongate/bladed clasts from each sample site were plotted on equal-area lower hemisphere Schmidt nets. These data were then computer contoured with a continuous Gaussian weighting function (kurtosis=100), producing the same expected count as a 1 percent counting circle (Robin and Jowett, 1986). Sample sites along the same levee that had similar flow directions (within 30

degrees) were grouped together. Fabric shape and strength were also described by the Spheristat program. Shape was defined by girdles or clusters. Scattered plots with no preferred orientation indicated weak fabric, while well-formed girdles or clusters indicated strong fabric. An eigenvalue ratio graph was constructed to show shape and strength of the fabric. To summarize imbrication, the percent of the total number of imbricated elongate/bladed and platy clasts was calculated. Dip-angle frequencies for imbricated clasts were displayed graphically for both elongate/bladed and platy clasts.

In order to obtain a quantitative analysis of the stereonets, the three-dimensional eigenvalue method was employed (Mark, 1973, 1974). The Spheristat program produced three eigenvalues τ_1, τ_2, τ_3 and their associated, mutually perpendicular eigenvectors V_1, V_2, and V_3 (Stesky and Pierce, 1990). V_1 represents the axis of maximum concentration of the long axes and V_3 the axis of minimum concentration. Mills (1984) points out that V_3 is the pole to the preferred plane of the long axis. According to Mark (1973), stereonet patterns with non-orthorhombic symmetry (axes that are not mutually perpendicular) may yield misleading results and should be interpreted with caution. The Spheristat program indicated whether each stereonet was non-orthorhombic. Non-orthorhombic nets were distinguished

from orthorhombic nets in eigenvalue analysis and interpretation.

Eigenvector analysis produces the quantities $S_1>S_2>S_3$ that indicate the degree of clustering of the axes about the eigenvectors V_1, V_2, and V_3, and are computed by dividing the eigenvalues by the total number of readings, N. The S_1 and S_3 values were produced for the debris-flow deposits to measure their mean strength. Tables provided by Mark (1973, 1974) allowed S_1 and S_3 values to be tested to determine whether V_1 and V_3 are significantly different from the values expected from a random sample of axes taken from a uniform population.

Mills (1991) analyzed the quantities $A_{0\text{-}90}$ and $A_{0\text{-}180}$, the mean absolute differences between the orientation of V_1 and the local flow direction, in order to compare the orientation of clasts from different studies. $A_{0\text{-}90}$ shows whether clast long-axes tend to be aligned parallel to flow (values near 0 degrees) or transverse to flow (values near 90 degrees). Where clast long-axes are parallel to flow (A0-90<20), $A_{0\text{-}180}$ shows if they dip upflow (values near 180 degrees) or downflow (values near 0 degrees) (Mills, 1991). To determine if the fabric of the Sacajawea debris-flow deposits is oriented more parallel or transverse with respect to flow direction, and whether parallel clasts dipped upflow or downflow, respective $A_{0\text{-}90}$ and $A_{0\text{-}180}$ values were computed, and then compared to $A_{0\text{-}90}$ and $A_{0\text{-}180}$ values

from other published debris-flow studies. The mean dip of V_l, referred to by Mills (1984) as D_l, was also computed.

Clast Size, Roundness, and Lithology

In order to characterize the coarser fraction of the deposits, clasts larger than 64 mm (cobble-size) were measured within grids on levees and lobes. Grids were placed every 20 meters along the most continuous levees. The length of the long-axis was recorded for at least 15 clasts at each site. The mean of the 10 largest clasts at each site was calculated to produce an overall mean for levees and each type of lobe.

Also recorded in each grid were roundness and lithology. Roundness was visually estimated using a roundness chart (Lindholm, 1987, p. 111). Lithologies were lumped into three groups: (1)Lodgepole limestone; (2)Three Forks silty and brecciated limestone and Sappington calcareous siltstone and sandstone; (3)Jefferson dolomite and limestone.

Although the overall size range was not studied, the percent clay, silt, and sand were determined by sieve and hydrometer analysis in order to characterize the finer portion of the deposits. One sample of finer material was collected from the bottom of a deposit, analyzed, and used to represent all of the finer material.

Grading

The presence or absence of graded bedding in vertical exposures was noted. If grading was present, it was determined to be either normal or reverse. Sketches were made and photos taken in vertical exposures of the deposits to document the presence or absence of sedimentary structures.

Talus Deposits

Fabrics and textures were documented for talus deposits in Sacajawea cirque. The surface of the deposits was examined to distinguish those which were matrix- and clast-supported. Three grids were set up on the talus in order to document fabric and clast size on the upper, middle and lower part of the slope. A total of 150 clasts were measured for orientation, according to the criteria described previously. Slope direction was also recorded. Three stereonets were produced by the Spheristat program and analyzed by the eigenvalue method. The S_1 and S_3 values were computed for the talus, as well as the $A_{0\text{-}90}$ and $A_{0\text{-}180}$ values. Dip angle and frequency of imbricated clasts were also analyzed. The 150 clasts were measured for size and roundness and lithology was recorded, following the methods described previously.

DEBRIS-FLOW DEPOSITS

Geomorphic Characteristics

Plates 1 and 2 show the channels and types of deposits mapped on oblique photos of the debris-flow fan. Many of the same features are mapped on both Plates 1 and 2, but due to the angle of the oblique photos, some of the features were mapped only on one or the other of the plates. There were a total of nine channels mapped; however, only six were chosen for geomorphic and sedimentologic analysis because they had distinct levees and the channels were not partially covered with soil and vegetation. These channels were numbered 1 through 6 as indicated on Plates 1 and 2. Also shown on Plates 1 and 2 are the rock units which outcrop above the debris-flow fan. The following section describes and interprets the deposit types and channel characteristics found.

Debris-flow Fan

Description. Five of the six channels on the debris-flow fan are fed by a main gully incised into bedrock above the fan apex. The area of this gully or drainage area is 0.006 km^2. The mouth of the gully (Plates 1 and 2) is steep (29 degrees) and has walls as high as 2 meters. Further up

the gully the steepness increases to approximately 35 degrees. The floor of the gully is covered with large clasts along its entire length, and in some reaches in-channel lobes block the floor of the gully.

Interpretation. The Sacajawea cirque fan is representative of fans in other alpine regions in that it is steep. The main gully or drainage area is also steep. Slopes ranging from 10 to 30 degrees have been reported for debris-flow fans in alpine regions of Scandinavia (Rapp and Nyberg, 1981) and Canada (Owens, 1973). Drainage areas contributing to debris-flow fans in alpine regions have slopes which are reported to range from 33 to 41 degrees (Curry, 1966). In contrast, arid debris-flow fans in Owens Valley, California have slopes ranging from 3 to 5 degrees and drainage areas that range from 6 to greater than 30 degrees (Whipple and Dunne, 1992).

The small size of both the Sacajawea cirque fan and the contributing main gully or drainage are smaller than other debris flow systems described in the literature. Fans studied in the Appalachians cover as much as 1.0 km^2 in area (Kochel, 1990), whereas drainage areas in Japan are larger than 0.5 km^2 (Ono, 1990). Harvey (1992) noted that when climate and geology are held constant, small, steep drainage basins tend to produce debris-flow dominated fans and larger, less steep basins produce fluvially dominated fans. Thus, size of a drainage area is an important factor which

appears to control the type of fan (Ono, 1990). The size of the Sacajawea cirque drainage area is important because it shows that a well-formed fan with well-developed debris-flow deposits can be constructed from a smaller drainage area than has previously been reported.

The main gully contributing to the debris-flow fan is located within the Three Forks and Sappington Formations. On its southwest side it is bounded by Three Forks brecciated limestone, while on its northeast side it is bounded by talus slopes from the Lodgepole formation. The brecciated limestone is a stripped structural surface which has been uncovered by gully erosion. This surface prevents further erosion by the gully because it is resistant limestone which dips towards the gully. Gully erosion has thus migrated in the direction of the dip of the less mechanically and chemically resistant calcareous siltstone and sandstone and shale units. It has undercut the basal shale of the Lodgepole, resulting in talus slopes which cover much of the Sappington unit. Gully erosion has also deepened the gully, under which less resistant Three Forks silty limestone and Sappington shale are also found. Thus, the presence of a stripped structural surface, the dip direction of this surface, and less resistant rock units in the cirque wall determined the location of the debris-flow drainage area.

Debris-flow Deposits

Description. Deposits can be subdivided into channel-related (levees and lobes) and open fan (overlapping, weathered lobate, and lobate) types (Plates 1 and 2). Levees are distinctively coarse textured and are continuous along many of the channels (Figure 5). At the base of the fan, the levees thin and spread out into terminal lobes (Figure 6) which block the mouths of the channels. Observation of terminal lobes shows they are thin, appear to contain fewer large clasts, and are spread out over a greater area than other types of lobes. Within some of the channels are very coarse-grained in-channel lobes (Figure 7) with steep lobate snouts. Along some channel margins, lateral lobes (Figure 8) have overtopped the levees. These lobes also have steep, lobate snouts.

Levees contain cobble-size clasts and their heights average 0.5 meters while widths vary from 0.3 to 1.2 meters (Table 2). Terminal lobes also contain predominately cobble-size clasts and are usually less than 0.2 meters thick. Some of the boulder-size clasts in in-channel lobes may be as large as 1.3 meters in length. Lateral lobes contain boulder-size clasts and may be as thick as 0.65 meters.

Deposits found on the open fan surface and not associated with the mapped channels include overlapping

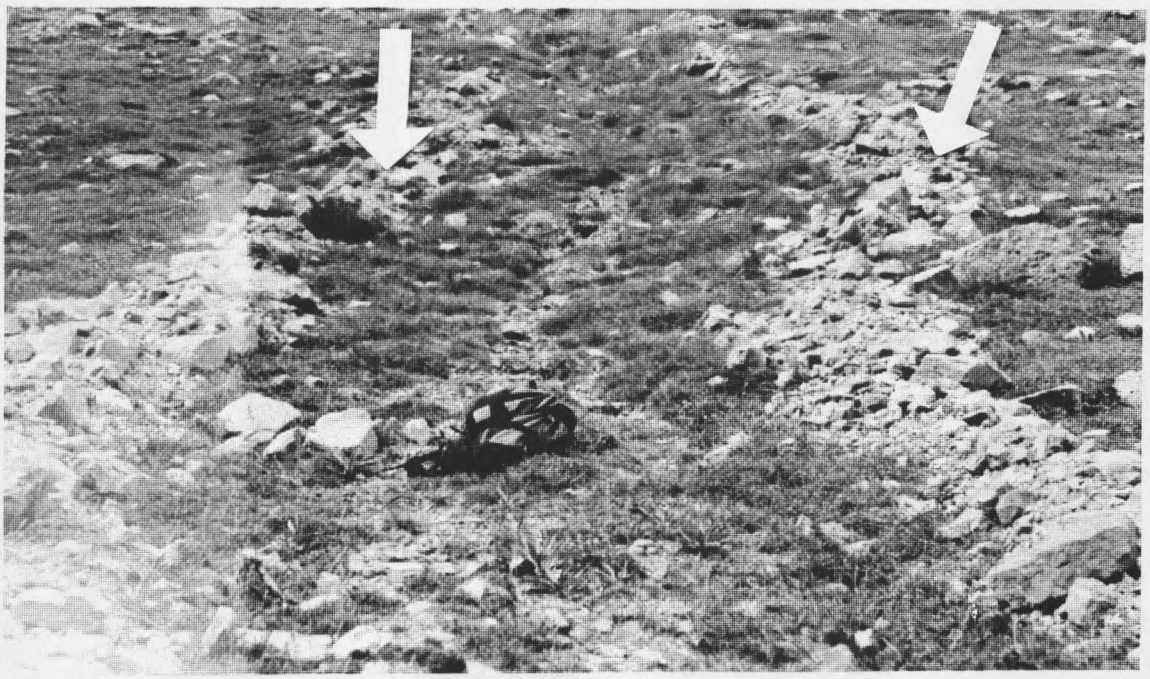

Figure 5. Two levees outlining Channel 3. View is upfan. Arrows point to levees. Backpack for scale.

Figure 6. Terminal lobe extending from a levee of Channel 3. Arrow points to upfan edge of lobe. Backpack for scale.

Figure 7. In-channel lobe blocking Channel 1. Arrow points to lobe front. Backpack for scale.

Figure 8. Lateral lobe that has spilled out of Channel 3 and partially covered a bush. Arrow points to front of lobe. Backpack for scale.

Table 2. Deposit types, descriptions, and interpretations.

Deposit	Description	Interpretation
Levees	Contain cobble-size clasts, height of 0.5 m, width 0.3-1.2 m.	Linear ridges deposited along sides of channels as flow advances.
Terminal Lobes	Contain cobble-size clasts, deposits less than 0.2 m thick, spread out laterally at mouth of channel.	Lobate forms deposited at mouth of channel by the front of the flow.
In-channel Lobes	Contain boulder-size clasts, lobes have steep fronts and sides, clasts are as large as 1.3 m in length.	Lobate forms deposited in the channel by flows that dewatered before travelling downfan.
Lateral Lobes	Contain boulder-size clasts, deposits as thick as 0.65 meters, lobes have steep fronts and sides.	Lobate forms diverted out of channel by in-channel blockage and deposited off the sides of the channel.
Overlapping Deposits	Thick deposits with an undulating surface that accumulated in two areas on the fan.	Accumulations of lobes and levees at mouth of main gully and north of Channel 1.
Weathered Lobate Forms	Lobes with steep snouts and clasts as large as 1 m in length. Weathering signs include pitted appearance of clasts, presence of lichens and partial burial of deposit.	Older in-channel or lateral lobes that have become partially buried by successive flows that built up the fan surface.
Lobate deposits	Lobate deposits that are not found on open fan surface. Contain cobble-size clasts.	Lobes that spilled out of area of overlapping deposits onto the upper fan.

deposits, weathered lobate forms, and lobate deposits (Plates 1 and 2). Overlapping deposits were mapped at the mouth of the main gully feeding the fan and on the north side of Channel 1. These deposits are termed overlapping deposits because individual levees and lobes cannot be distinguished in these deposits. They have a higher surficial topography relative to the other deposits on the fan. This implies that many deposits have accumulated at these sites.

Weathered lobate forms are found between Channels 3 and 4 and on the north side of Channel 1. These deposits have distinctive lobate forms with steep snouts and clasts as large as 1 meter in length. There are signs of weathering such as the pitted appearance of the dolomite and limestone clasts as well as the presence of lichens on the clasts. Each weathered lobate form is also partially buried by subsequent levees and lobes.

Lobate deposits are found on the upper fan surface between the channels (Plates 1 and 2). Because they show no relation to the surrounding channels, it is not clear what type of lobe they are. Thus, they were termed lobate deposits because they are distinctly lobate.

Interpretation. Levees, terminal lobes, lateral lobes, and in-channel lobes are the most common types of debris-flow deposits recognized (Sharp, 1942; Johnson and Rodine, 1984; Costa, 1984). Overlapping deposits are accumulations

of lobes and/or levees. They accumulated at the mouth of the main gully because some flows stopped in this area and did not travel downfan. Weathered lobate forms are older in-channel or lateral lobes that have become partially buried by successive flows that built up the fan surface. Lobate deposits represent lobes that spilled over the area of overlapping deposits and were deposited on the upper fan surface between the channels. Deposits such as these show no association with the channels and are found on the open fan surface. Similar deposits have also been recognized by Whipple and Dunne (1992) in Owens Valley, California, and termed boulder fields. They are thought to represent partially buried or morphologically degraded overbank debris-flow lobes (Whipple and Dunne, 1992).

Channels

Description. The channels present on the fan vary in size (Table 3), shape, and the types of deposits associated with them. The heads of all the channels begin below the area of overlapping deposits described previously. The area of overlapping deposits blocks the main gully from connecting directly with any one channel.

Channel 1 is the largest and deepest channel (Table 3) present on the fan and has a well-developed U-shaped cross-section. During summer months, a constant stream flow runs through this channel. Channel 1 has the largest and most

Table 3. Channel lengths, mean widths, and mean depths.

Channel	Length (meters)	Mean Width (meters)	Mean Depth (meters)
1	150	5.9±0.9	2.1±0.1
2	127	3.1±0.1	0.8±0.1
3	131	4.1±0.2	0.5±0.1
4	88	3.0±0.2	0.8±0.1
5	76	4.4±0.4	0.9±0.1
6	117	3.0±0.2	0.4±0.1

continuous levees (Plate 1). Along some stretches of the channel, compound levees are found side-by-side. Three distinct lateral lobes are found on the sides of Channel 1. There are no terminal lobes found at the mouth of Channel 1. Channel 1 contains three in-channel lobes at the top of the fan. Two older channels extend from the north side of Channel 1. These two channels were not studied in detail because they are overgrown with vegetation and their levees are very discontinuous and poorly preserved. However, they can be recognized morphologically and were included on Plates 1 and 2.

The floor of Channel 2 is shallow (Table 3) and covered with vegetation similar to vegetation found on the open fan surface. The center of the channel is incised and V-shaped. Channel 2 has levees that are as narrow as 0.3 meters and discontinuous in the mid-fan region. Three lateral lobes extend off the sides of the channel. There are no in-

channel lobes. At the mouth of Channel 2, a thin, terminal lobe spreads out. The terminal lobe was deposited on top of a bush, as the bush can be seen poking up through the middle of the lobe and on either side of it. The lobe also covered a hiking trail.

Like Channel 2, Channel 3 has vegetation on the channel floor, with only the very center showing the V-shaped incision. The levees on the sides of Channel 3 are continuous and widen at the toe of the fan into a terminal lobe that is thin and adjoins the terminal lobe of Channel 2. There are two lateral lobes associated with Channel 3, one of which is deposited on top of part of a large bush in the center of the fan. No in-channel lobes are present.

Channel 3 and Channel 4 begin from the same entrenched channel. The channel floor is covered with vegetation. The center is incised and V-shaped. The most distinctive feature of Channel 4 is the four in-channel lobes that plug the narrow channel and in some areas spread out over the sides of the channel. Levees are continuous where the in-channel lobes have not spilled out of the channel. Three large lateral lobes extend off the side of the channel. At the mouth of the channel, thin terminal lobes are found, although their lobate form is less conspicuous than the terminal lobes of Channels 2 and 3.

Channel 5 is well-defined only in the mid-fan area. In its upper reaches and at the base of the fan, the channel is

partially overgrown with vegetation and difficult to follow where there are no levees. Its most continuous reach is narrow and shallow (Table 3). Channel 5 has well-defined levees but no lobes of any type can be discerned. The floor of the channel is U-shaped and covered with clasts. On the west side of Channel 5 is another channel, barely visible, which extends from a narrow gap between the Jefferson and Three Forks Formations, and not from the main gully. This channel was not studied in detail because it is filled with vegetation and has very few levees.

Channel 6 has its source in a small gully between outcrops of Jefferson dolomite and limestone. Although Channel 6 does not extend from the main gully, it was chosen for study because it is proximal to the fan and has well-formed and continuous levees. Channel 6 is the most narrow and shallow channel (Table 3). Continuous levees outline the shallow but U-shaped channel floor. A pronounced terminal lobe is found at the mouth of the channel. However, no other types of lobes are present.

Interpretation. The channels on the Sacajawea cirque fan are both U- and V-shaped. Owens (1973) found U-shaped channels to be more typical of alpine debris flows in Canada, yet V-shaped channels were also reported. The lengths of the channels on the debris-flow fan are shorter than those cited in the literature. The debris-flow channels on the Sacajawea cirque fan range from 88 to 150

meters long, whereas in Scandinavia measured channel lengths ranged from 181 to 1800 meters long (Rapp and Nyberg 1981).

The source area of Channel 6 is not a narrow gully filled with large clasts, but rather a steep, smooth hillslope between outcrops of the Jefferson Formation. A gully was not able to form in the Jefferson Formation because dolomite and limestone beds are resistant to both mechanical and chemical weathering in the relatively arid Montana climate (Locke and Lageson, 1989). Thus, debris flows can be initiated on smooth, steep hillslopes as well as in narrow gullies, and still form the well-developed lobes and levees displayed in Channel 6.

The greater width and depth and number of lobes along Channel 1 than the other channels suggest it has been the most active channel in the past; however, its large size may also be due to incision by running water during the spring and summer months. The most recently recognized flows occurred in 1987 (Jim Schmitt, personal communication), when they formed Channels 2 and 3 and covered a hiking trail and several bushes. These were isolated events. There is no evidence such as numerous lobes or compound levees which would indicate prior or subsequent flows had gone down these channels. As the area of overlapping deposits blocks the main gully from connecting with any one channel, which channel the next flow takes appears random.

Channel Profiles

Description. Channels 1 and 4 possess in-channel lobes blocking the channel at various stretches. The in-channel lobes along a channel produce a step-like channel floor (Figure 9).

Interpretation. The channel profiles illustrate the step-like character of the channel floors which are created by in-channel lobes which block certain reaches of the channel. Whipple and Dunne (1992) noted that on debris-flow fans, in-channel lobes block channels and at each lobe, a new elevation of the channel floor is created. As a result, subsequent flows moving down the channel are diverted out of the channel upon reaching the channel blockages. Though what channel a flow takes is random, encountering an in-channel lobe may divert a flow out of a channel, thus affecting the pattern of deposition on the fan.

Sedimentologic Characteristics

Clast Packing

Description. The debris-flow deposits are clast-supported (Figure 10), with particles pebble-size and larger (>4 mm) touching and only the voids filled with matrix. Sampling of the matrix revealed that it is made up of predominately granule-size particles (2 mm-4 mm) and less finer material. Overall, there is little matrix. The

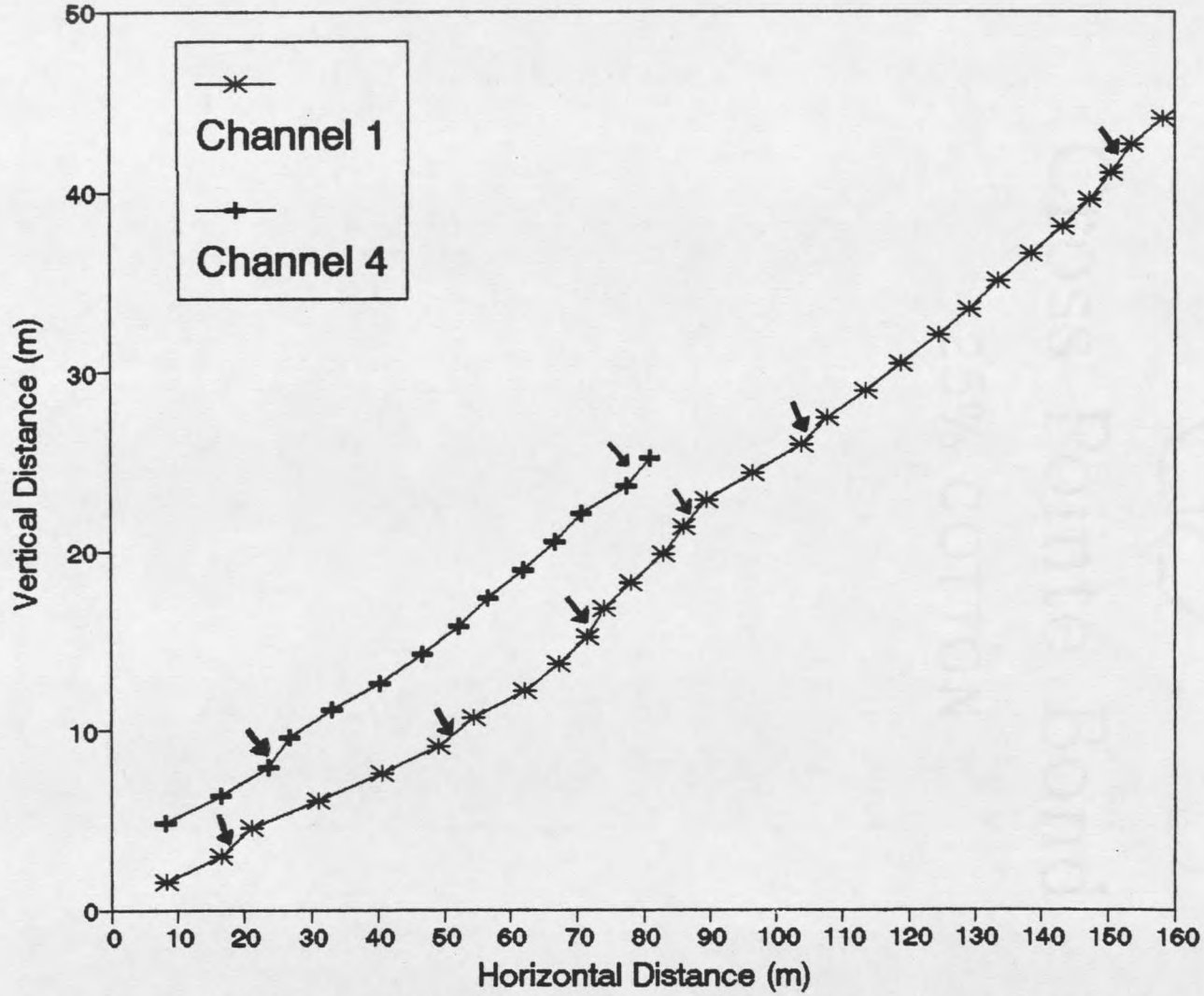

Figure 9. Channel profiles of Channels 1 and 4. Arrows point to location of channel blockages. Vertical exaggeration=4X.

surface of the levees and lobes is coarse, with the matrix observable only upon digging less than 0.5 meters beneath the deposit surface.

Figure 10. Clast-supported framework of pebble and larger-size clasts in an exposed vertical section of a levee in the main gully. Pencil for scale.

Interpretation. Matrix-supported fabric is cited as a common characteristic of debris-flow deposits (Smith, 1988; Costa, 1988; Eyles and Kocsis, 1988; Hubert and Filipov, 1989). Though many debris-flow deposits are clast-supported, this has not been recognized as a common characteristic in the literature (Sharp and Nobles, 1953; Curry, 1966; Lowe, 1979b; Shultz, 1984; Mills, 1984; Tanner and Hubert, 1991). In many debris flows, the largest clasts

are not actually suspended within a clay matrix, but remain in contact with one another while rolling, sliding, and bouncing downslope (Lowe, 1982). The clay matrix serves to lubricate the grains rather than support them as in matrix-supported debris flows. As a result, they leave deposits that are clast-supported. Flows of this type have been described by Sharp and Nobles (1953), Curry (1966), Lowe (1979b), Shultz (1984), Mills (1984), and Tanner and Hubert (1991). The deposits of debris flows with a clast-supported framework include a small proportion of clay, sometimes as little as 5% of the flow by volume (Rodine and Johnson, 1976). Though the overall percent of clay in the deposits in Sacajawea could not be determined due to large samples needed for measurement, it most likely was small due to the lack of finer matrix in the deposits. Thus, clast-supported deposits should also be considered a common fabric characteristic of debris-flow deposits.

The clast-support framework of the Sacajawea debris-flow deposits is due to the relative abundance of large clasts (pebble-size and larger) in the source area. The larger clasts are primarily calcareous siltstone and limestone which are hard to break down into finer silt- and clay-sizes. Also, Rappol (1985) noted that there is an abundance of pebble through boulder sizes in bedrock-rich alpine regions.

Although the overall amount of fines in the deposits was determined by trenching to be small, during flow initiation there was undoubtedly more finer material present to lubricate the grains and initiate flow. This is because the main gully is on top of Three Forks and Sappington shale, calcareous siltstone and sandstone, and silty limestone which break down into finer materials by weathering in place. One explanation of where the finer materials in the deposits went is washing of the clasts after deposition. Curry (1966) and Blair and McPherson (1992) observed this phenomena and suggested that the fine material originally on the surface of the deposits drained or washed away sometime after the flow came to rest and is present beneath the surface boulders. This mechanism likely explains the coarse surface of the deposits noted in this study; however, it does not explain the lack of finer material beneath the deposit surface.

Clast Fabric

Description. Contoured Schmidt nets reveal the orientation pattern of clasts in sampled levees (Figure 11). Sample sites are shown on Plates 1 and 2. Because Channels 1 and 6 are oriented in different directions on the fan, the sample sites on the levees are also noted by different directions. Although there is scatter of data points, according to the Spheristat program, the stereonets for

levees show weakly developed girdles, except for the Channel 6 east side b levee which shows a moderately developed girdle and cluster. Clasts are oriented parallel to flow and dipping downstream. Dip of the clasts ranges from 10 to 25 degrees. A few clasts have dips greater than 50 degrees (Appendix A).

Six contoured Schmidt nets were created for the in-channel, lateral, and terminal lobes that were sampled (Figure 12). Sample sites are shown on Plates 1 and 2. Scatter is greater in the lobes than in the levees. The stereonets for the lobes show weakly developed girdles and clusters with clasts oriented parallel and oblique to flow and dipping both up and downstream. There is a wider range of dips of clasts in lobes than in levees, ranging from 2 to 72 degrees (Appendix A). Dips are lower for terminal lobes than for in-channel and lateral lobes.

Imbrication is more prevalent in platy clasts than in elongate/bladed clasts. Overall, imbrication is minor in the deposits, as less than fifty percent of clasts are imbricated: twenty-five percent of platy clasts are imbricated, while only eleven percent of elongate/bladed clasts are imbricated. Of all the different types of deposits, lateral lobes have the greatest percentage of imbricated clasts. Sixty-seven percent of the platy imbricated clasts are from lateral lobes (Appendix B).

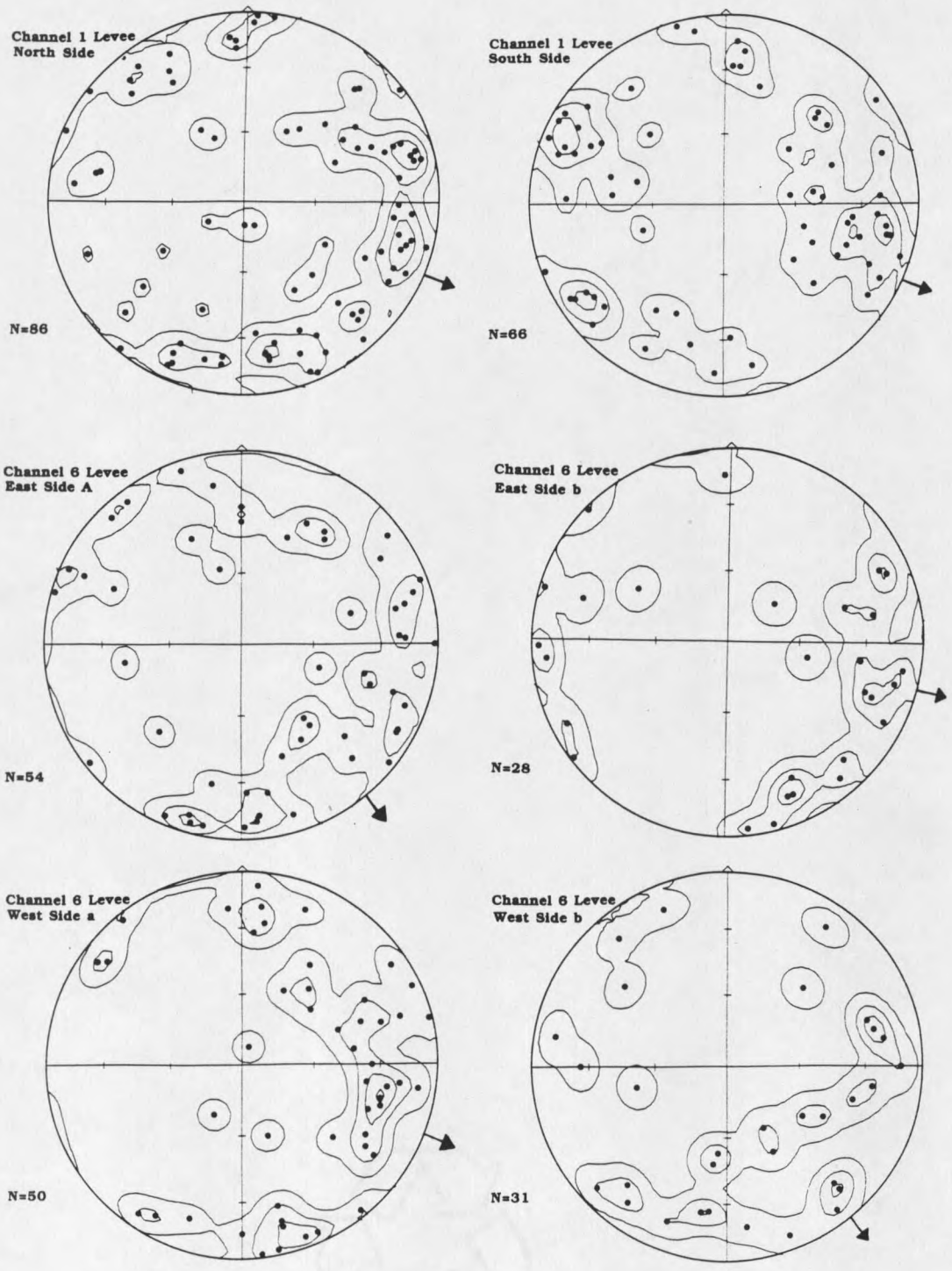

Figure 11. Contoured lower hemisphere Schmidt nets of sampled levees showing orientation of clasts with respect to downflow channel direction (given by arrows).

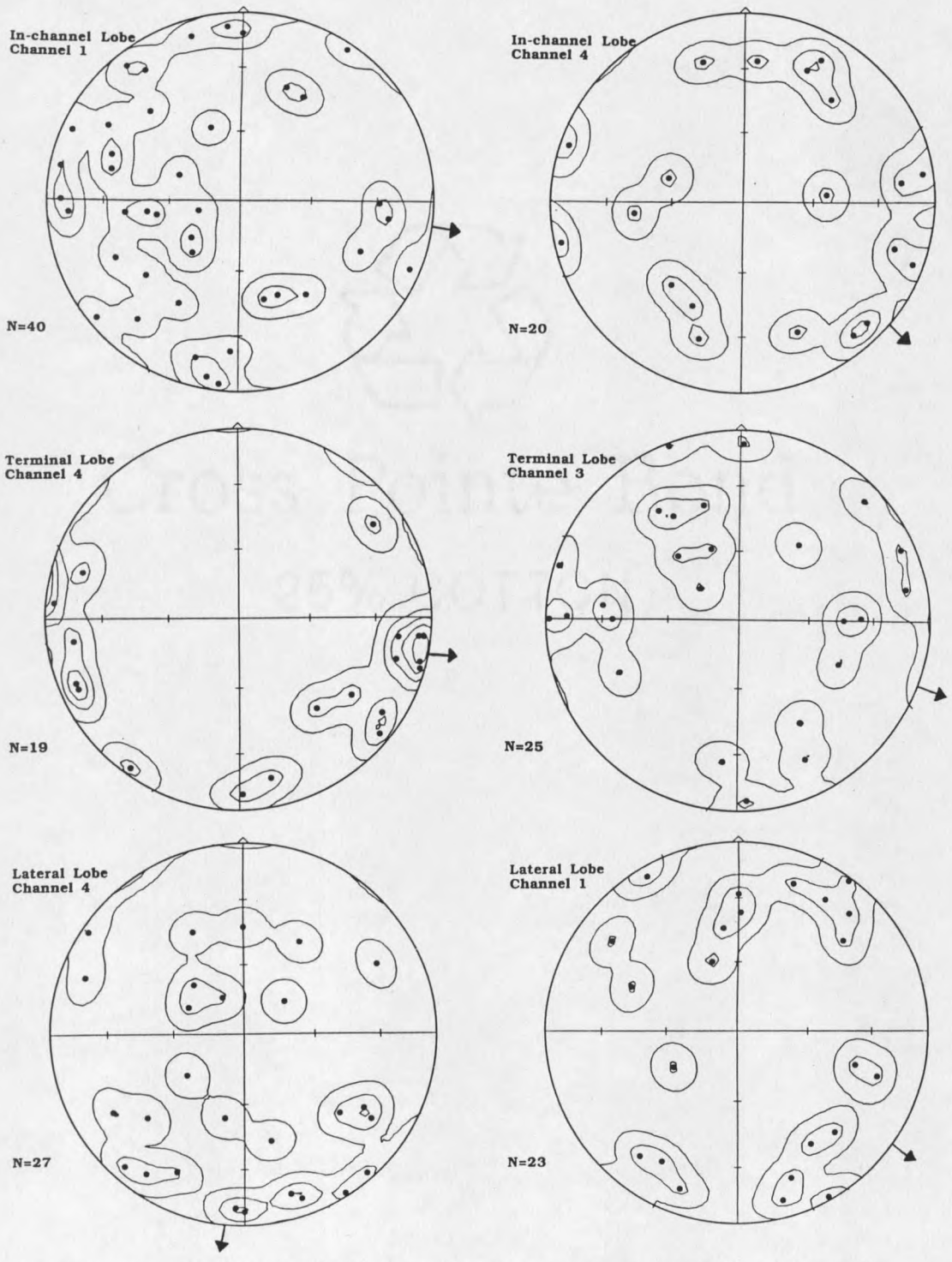

Figure 12. Contoured lower hemisphere Schmidt nets of sampled lobes showing orientation of clasts with respect to downflow channel direction (given by arrows).

Dip-angle frequencies for platy and elongate/bladed clasts are shown in Figure 13. The highest dip-angle frequency for elongate/bladed clasts is for dips ranging from 0 to 9 degrees. Platy clasts show high dip-angle frequencies for dips ranging from 20 to 29 and 40 to 49 degrees.

Interpretation. Comparison of these fabric patterns with other published data shows that there are some common characteristics of debris flow fabrics, including scatter of data points, weakly developed girdles, and a dominance of parallel orientation. However, there is more variability of dip angle among debris flow studies. Many authors cite dips less than 10 degrees (Eyles and Kocsis, 1988; Hubert and Filipov, 1989; Tanner and Hubert, 1991), while this study and Owens (1973) found dips were higher. In studies where fabric of levees and lobes was discussed, there were some differences from this study. In debris flows studied in Owens Valley, California, elongate/bladed clasts in levees showed parallel orientations but upflow dips of clast long-axes, while in lobes clasts were subparallel to flow with steep upflow dips (Hubert and Filipov, 1989). In alpine debris flows in Canada, clasts in levees showed parallel orientations and downstream dips, while clasts in lobes showed strong transverse orientations (Owens, 1973). A quantitative comparison between this study and others where

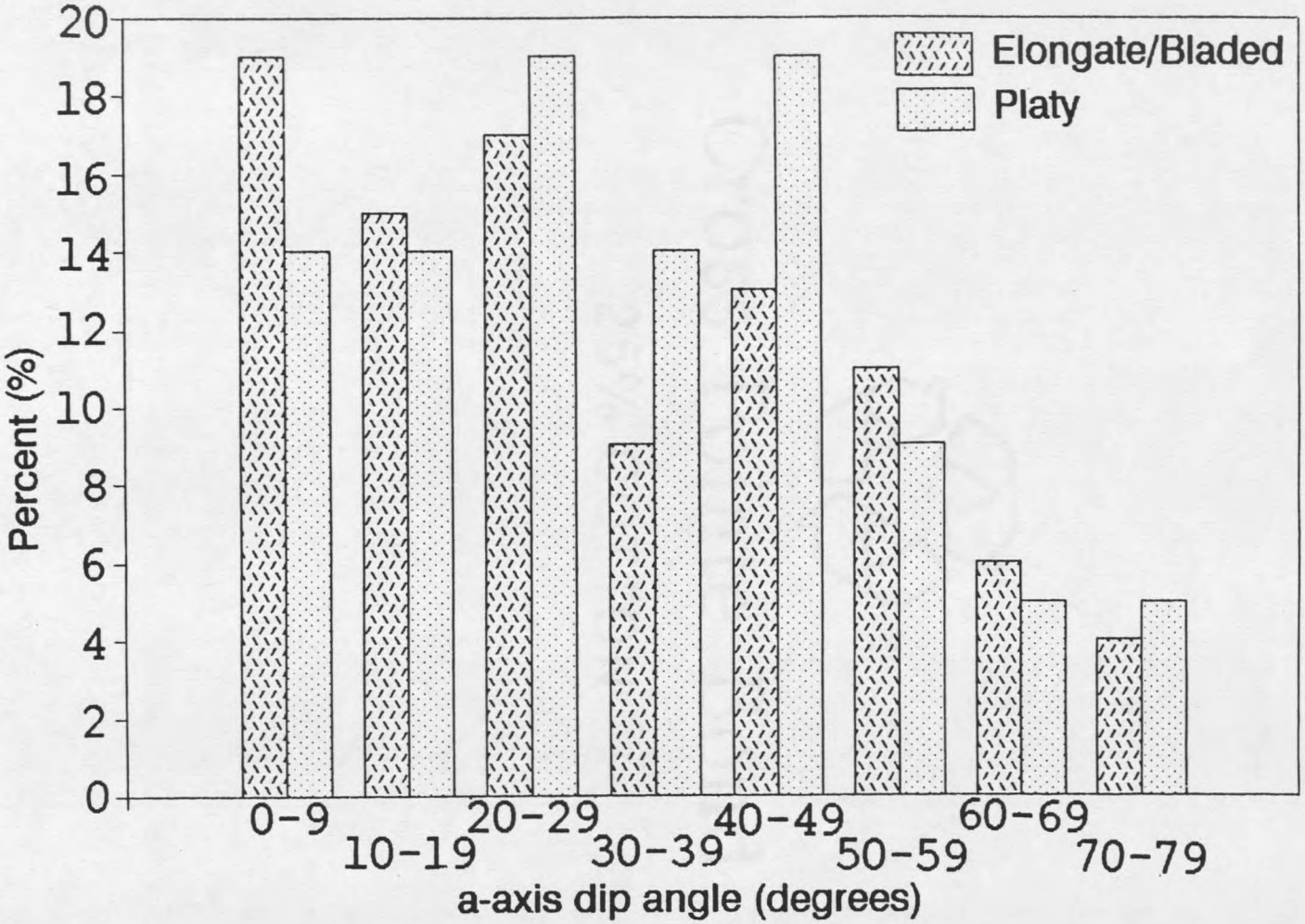

Figure 13. Histogram of dip-angle frequencies for imbricated elongate/bladed and platy clasts from levees and lobes.

the eigenvalue method was employed (below) allows a more rigorous comparison of results.

Imbrication was found to be minor in the Sacajawea debris-flow deposits. Minor imbrication in debris flows has also been recognized by Shultz (1984) who noted that 15% of elongate clasts were imbricated. Johnson and Rodine (1984) also noted more platy clasts showed imbrication than did elongate/bladed clasts and that platy clasts dipped away from the edges of lobes at steep angles. The shallow inclination of elongate clasts has also been documented elsewhere (Rappol, 1985; Eyles and Kocsis, 1988).

Eigenvalue Analysis

Description. The eigenvalue method (Mark, 1973, 1974) was used to quantitatively analyze the twelve samples, including six levees and six lobes (see Glossary for review of eigenvalue terminology). Table 4 summarizes the eigenvalue analysis of the twelve samples. Four of the samples (those marked with an asterisk) were determined by the Spheristat program to be orthorhombic. All six levees have V_1 azimuths within 30 degrees of a downstream orientation, while only two of the lobes show V_1 azimuths within 30 degrees of a downstream orientation (Channel 4 lateral lobe; Channel 4 terminal lobes). Two of the lobes have V_1 azimuths within 30 degrees of an upstream direction or upstream imbrication (Channel 1 in-channel lobe; Channel

Table 4. Summary of eigenvalue analysis of clast fabric for the Sacajawea cirque debris-flow deposits.

Sample	n	Flow Dir.	V_1 Azi.	V_1 Dip	S_1	S_3
Ch 6 Lev West b	31	141	144	29	0.47	0.17
Ch 1 Lev South	66	112	96	10	0.50	0.23
Ch 6 Lev East a	54	140	130	15	0.47	0.15
Ch 6 Lev East b	28	104	109	14	0.61	0.12
Ch 1 Lev North *	86	111	127	18	0.47	0.17
Ch 6 Lev West a*	50	108	111	30	0.48	0.11
T Lobe Ch 4	19	100	101	6	0.70	0.04
T Lobe Ch 3 *	25	109	299	15	0.44	0.23
Lat Lobe Ch 4	27	184	169	15	0.44	0.25
Lat Lobe Ch 1	23	124	0	7	0.52	0.21
I-c Lobe Ch 4	20	129	90	5	0.44	0.21
I-c Lobe Ch 1 *	40	98	266	34	0.44	0.20

* Orthorhombic samples
Note: Values for flow direction, V_1 azimuth and V_1 dip are in degrees.

3 terminal lobe). Finally, two lobes have V_1 azimuths oblique to flow (Channel 4 in-channel lobe; Channel 1 lateral lobe).

S_1 and S_3 values, which provide a measure of mean fabric strength, are also displayed in Table 4. Overall, the deposits have weak fabric (S_1<0.60), except for the Channel 6 east b levee and Channel 4 terminal lobe which have stronger fabric. Fabric strength of levees is stronger than that of lobes. Figure 14 is an eigenvalue ratio graph showing strength and shape of the twelve samples. This graph confirms that the Sacajawea cirque debris flows are characterized by weak fabric and girdle shape. Significance tests show that only six of twelve S_1 values and nine of twelve S_3 values are significantly different from random at the 0.05 level (Table 5).

The A_{0-90} and A_{0-180} values determined for the Sacajawea cirque debris-flow deposits are 15 and 47 degrees, respectively. The A_{0-90} value is close to 0, or a flow-parallel orientation. However, the standard deviation is 16, suggesting that the orientation can be oblique to flow as well. The A_{0-180} value, 47, is closer to 0 than 180, suggesting that clasts oriented parallel to flow dip downflow. However, the standard deviation is 65, suggesting that clasts may dip both up and downflow. The mean dip of the V_1 azimuth, D_1, is 17 degrees.

Interpretation. The orientations of the V_1 azimuths show that there is a preference for downstream orientation of clast long-axes, particularly in levees. The flow-parallel orientation is weak, however, because the strength

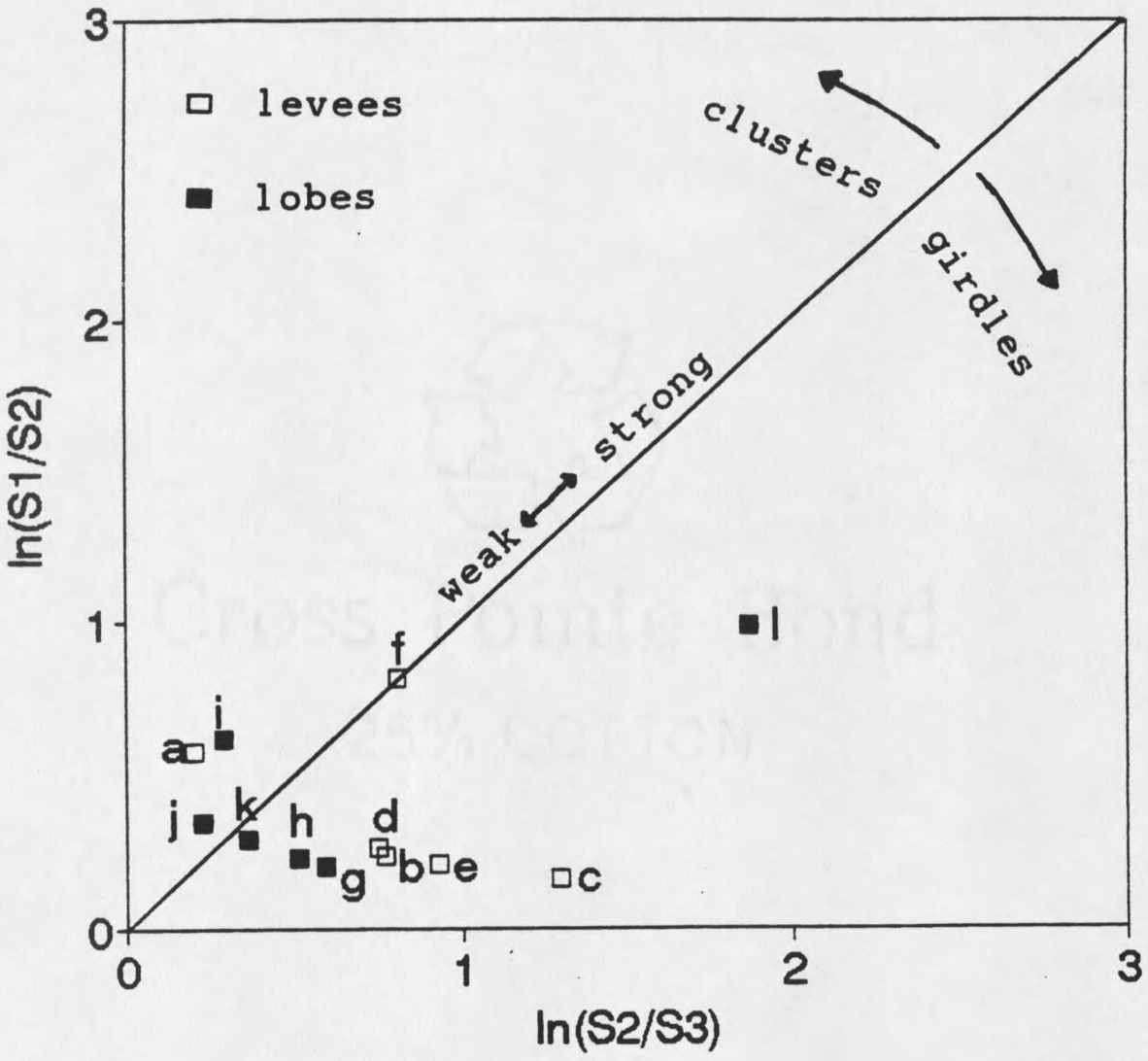

Figure 14. Eigenvalue ratio graph of normalized eigenvalues and their relationship to shape and strength of the debris flow fabric. Strength increases away from the origin of the diagram. Clusters fall above the center line, girdles fall below the center line. Levees are represented by a-f (a=Ch.1 south, b=Ch. 1 north, c=Ch. 6 West a, d=Ch. 6 West b, e=Ch. 6 East a, f=Ch. 6 east b). Lobes are represented by g-l (g=Ch. 1 in-channel, h=Ch. 4 in-channel, i=Ch. 1 lateral, j=Ch. 4 lateral, k=Ch. 3 terminal, l=Ch. 4 terminal). After Woodcock and Naylor (1983).

Table 5. Five percent significance levels (S.L.) for S_1 and S_3 from the debris flow samples relative to a random distribution.

Sample #	n	S_1	5% S.L.	Sig? y or n	S_3	5% S.L.	Sig? y or n
Ch 6 Lev West a	50	0.48	0.46	y	0.11	0.22	y
Ch 6 Lev West b	31	0.47	0.49	n	0.17	0.18	y
Ch 1 Lev North	86	0.47	0.43	y	0.17	0.24	y
Ch 1 Lev South	66	0.50	0.44	y	0.23	0.24	y
Ch 6 Lev East a	54	0.47	0.45	y	0.15	0.22	y
Ch 6 Lev East b	28	0.61	0.50	y	0.12	0.17	y
T Lobe Ch 4	19	0.70	0.54	y	0.04	0.15	y
T Lobe Ch 3	25	0.44	0.51	n	0.23	0.17	n
Lat Lobe Ch 1	23	0.52	0.53	n	0.21	0.17	y
Lat Lobe Ch 4	27	0.44	0.50	n	0.25	0.17	n
I-c Lobe Ch 1	40	0.44	0.47	n	0.20	0.21	y
I-c Lobe Ch 4	20	0.44	0.54	n	0.21	0.15	n

NOTE: A larger S_1 and a smaller S_3 indicate greater strength.

of the fabric is also weak. Clasts in lobes show more variation in orientation and dip than levees but there is no orientation unique to each type of lobe. Orientations parallel to flow are most commonly cited for debris flows

(Smith, 1986). However, debris flow deposits reported in the literature appear to show no preferred direction of dip (Mills, 1984).

The flow-parallel orientation of clasts in levees indicates laminar flow (Lindsay, 1968; Hampton, 1975; Enos, 1977; Smith, 1986). Innes (1983) and Owens (1973) found a preferred orientation of clasts in levees and no preferred orientation in lobes. Owens (1973) attributed the variable orientation in lobes to either turbulent flow in the lobes with fewer large clasts (such as terminal lobes) or reworking by running water of clasts in-channel lobes. Also, post-depositional settling processes such as solifluction might affect clasts in steep lobes, such as in-channel and lateral lobes.

Although fabric strength is weak overall for the Sacajawea cirque debris-flow deposits, the lobes are weaker than the levees as revealed by the S_1 and S_3 values. As previously mentioned, this may indicate turbulent flow within lobes. Lindsay (1968) reported that where turbulent flow occurs, a much weaker fabric develops.

Table 6 shows the mean values of S_1 and S_3 for the Sacajawea cirque debris flows compared to other debris flow studies where the eigenvalue method was employed. The Sacajawea cirque debris flows have the lowest S_1 values and highest S_3 values, indicating the weakest fabric reported for debris flows.

Table 6. Comparison of S_1 and S_3 values from selected debris-flow studies.

Debris-Flow Study	N	S_1	S_3
Sacajawea cirque Debris Flows (all samples)	12	0.50* 0.07**	0.17 0.06
NF St. Helen's Lahars (matrix-supported) (Mills, 1984)	6	0.57 0.08	0.15 0.04
NF St. Helen's Lahars (clast-supported) (Mills, 1984)	5	0.56 0.07	0.13 0.04
SW St. Helen's Lahars (Major & Voight, 1986)	12	0.52 0.06	0.14 0.05
Alpine Debris Flows Germany (Rappol, in Mills, 1991)	12	0.62 0.07	0.11 0.05
Pleistocene Debris Flows Canada (Rappol, 1986)	3	0.55 0.03	0.13 0.02
Debris Flows, Sweden (Nyberg, in Mills, 1991)	3	0.55 0.08	0.14 0.03
Alpine Debris Flows Canada (Owens, 1972)	84	0.61 0.08	0.10 0.04

* Sample mean ** Sample standard deviation

Table 7 shows the results of significance tests ($p<0.05$) on S_1 and S_3 values. The S_1 and S_3 values for the Sacajawea cirque debris flows differ significantly from alpine debris flows in Germany (Rappol, 1986) and Canada (Owens, 1973) but not from North Fork St. Helen's lahars (Mills, 1984), debris flows in Sweden (Nyberg, in Mills, 1991), or Pleistocene debris flows in Canada (Rappol, 1986).

Table 7. Significant clast fabric differences between the Sacajawea cirque debris flows and selected debris-flow studies.

Debris-Flow Study	Sacajawea cirque Debris Flows				
	A_{0-90}	A_{0-180}	D_1	S_1	S_3
NF St. Helen's Lahars (matrix-supported) (Mills, 1984)	*	*	-	-	-
NF St. Helen's Lahars (clast-supported) (Mills, 1984)	*	-	-	-	-
SW St. Helen's Lahars (Major & Voight, 1986)	*	*	*	NA	NA
Alpine Debris Flows Germany (Rappol, 1986)	NA	NA	NA	*	*
Debris Flows, Sweden (Nyberg, in Mills, 1991)	*	-	-	-	-
Pleistocene Debris Flows Canada (Rappol, 1986)	NA	NA	NA	-	-
Alpine Debris Flows Canada (Owens, 1973)	-	-	-	*	*

-= insignificant @ $p<0.05$ *= significant @ $p<0.05$
NA= not available
Note: The two-sample t-test was used to test the means of the values. It was assumed that the variance of the two populations represented by the samples were equal.

Although debris flows appear to have a wide range of S_1 values (from 0.50 to 0.62) (Table 6), when compared to other diamictons the range for debris flows is distinctive. Solifluction lobes in Alaska showed a mean S_1 value of 0.90 (Nelson, in Mills, 1991). Basal ice debris in Alaska was 0.85, while basal melt-out till had a mean S_1 value of 0.82

(Lawson, 1979a). Thus, the fabric strength of debris flows is noticeably weaker than the strength of diamictons such as till and solifluction lobes.

The A_{0-90} value for the Sacajawea cirque debris-flow samples, including both orthorhombic and non-orthorhombic samples, is 15 and the A_{0-180} value is 47. The large standard deviations of these values are caused by the great spread of the data due to inclusion of stereonets with multimodal data or non-orthorhombic symmetry in the calculations. When only the four orthorhombic nets are analyzed, the A_{0-90} value is 10 with a standard deviation of 5, or a flow-parallel orientation of clasts. The A_{0-180} value is 89 with a standard deviation of 68. According to Mills (1991), A_{0-180} values between 70 and 110 degrees and A_{0-90} values below 20 degrees indicate that the samples are roughly divided between upflow and downflow orientations. The values show 46% of the data from the four orthorhombic samples to be parallel to flow with half the clasts dipping downflow and half dipping upflow.

Table 8 shows A_{0-90} and A_{0-180} values of the Sacajawea cirque debris flows compared to those from other debris flow studies where a flow direction was given. The clast-supported lahars of the North Fork of the Toutle River at Mount St. Helens (Mills, 1984) show a strong transverse orientation, whereas the matrix-supported lahars show a parallel to oblique orientation. From these results, Mills

(1984) suggests that orientation pattern may be related to clast packing. The values for the Sacajawea cirque debris flows disprove this, as the deposits are clast-supported but show an overall parallel orientation of clasts. Alpine debris flows in Canada (Owens, 1973) also show a parallel orientation of clasts but no reference was made as to whether the deposits were matrix- or clast-supported. Oblique orientations are shown for clasts in Swedish debris flows (Nyberg, in Mills, 1991), while lahars of the Southwest Fork of the Toutle River at Mount St. Helens (Major and Voight, 1986) exhibit parallel and oblique orientations of clasts. Neither study discussed clast packing.

The A_{0-90} value of the Sacajawea cirque debris flows differed significantly from North Fork St. Helen's matrix- and clast-supported lahars (Mills, 1984), Southwest St. Helen's lahars (Major and Voight, 1986), and debris flows in Sweden (Nyberg, in Mills, 1991) (Table 7). The A_{0-180} value, on the other hand, differed only from the North Fork St. Helen's lahars (matrix-supported) and the Southwest St. Helen's lahars (Major and Voight, 1986).

According to Mills (1991), although A_{0-90} and A_{0-180} values represent the mean orientation and dip direction of all clasts from a study, they are useful when comparing orientations of clasts from different studies. However, all the A_{0-90} and A_{0-180} values listed for the studies in Table 8

Table 8. Comparison of A_{0-90}, A_{0-180}, and D_1 values from selected debris flow studies.

Debris Flow Study	N	A_{0-90}	A_{0-180}	D_1
Sacajawea cirque Debris Flows	12	15* 16**	47 66	17 10
NF St. Helen's Lahars (matrix-supported) (Mills, 1984)	6	37 22	143 21	13 5
NF St. Helen's Lahars (Clast-supported) (Mills, 1984)	5	65 30	109 28	15 10
SW St. Helen's Lahars (Major and Voight, 1986)	12	39 33	113 58	8 6
Debris Flows, Sweden (Nyberg, in Mills, 1991)	3	59 28	121 28	11 13
Alpine Debris Flows Canada (Owens, 1972)	84	21 21	35 47	15 8

*Sample Mean
**Sample Standard Deviation
Note: All values, except for N, are in degrees.

show large standard deviations, suggesting that clast orientations in debris flows are variable and that other debris-flow studies may have included non-orthorhombic stereonets in calculations, as none of the authors stated that non-orthorhombic stereonets were discounted. Mills (1991) used A_{0-90} and A_{0-180} values to compare orientations of different diamictons in studies where a slope or flow direction was given and found that most of the studies showed mean preferred orientations parallel or oblique to the flow or slope direction. This suggests that diamicton

are not well distinguished by fabric pattern. Rather, a fabric characteristic that distinguishes diamicton is mean fabric strength, or S_1 and S_3 values. This is because the variable orientation of clasts in a debris-flow deposit results in weak fabric which can be differentiated from diamictons that exhibit preferred orientations or strong fabric.

Table 8 also shows the D_1 value, or the mean dip of the V_1 eigenvector. The D_1 value for all the Sacajawea samples is 17 degrees, and although it is the highest value of all the debris flows, all the values for debris flows are low. The D_1 value for the Sacajawea cirque debris flows differs significantly only from the Southwest St. Helen's lahars (Major and Voight, 1986) (Table 7). According to Mills (1991), most debris flow fabrics have dips less than 15 degrees. Diamictons with exceptionally steep dips include basal-ice debris, talus, and rock glaciers (Mills, 1991).

Clast Size, Roundness, and Lithology

Description. The mean size of clasts larger than 64 mm in levees is 215 mm with a standard deviation of 45 mm. Lateral lobes have a mean clast size larger than 64 mm of 257 mm with a standard deviation of 21 mm, while in-channel lobes have a mean clast size larger than 64 mm of 271 mm with a standard deviation of 156 mm. Thus, the mean size of clasts larger than 64 mm in levees, lateral lobes, and in-

channel lobes ranges from cobble to boulder-size. Terminal lobes have a mean clast size larger than 64 mm of 174 mm with a standard deviation of 36 mm and thus are in the cobble-size range. Sample sites are shown on Plates 1 and 2.

The overall size range present in the deposits was not studied. The percentage of sand, silt, and clay in a sample of the matrix was determined by sieve and hydrometer analysis to be 36% sand, 54% silt, and 10% clay.

Forty-three percent of the clasts larger than 64 mm are subrounded. The remainder of the clasts are either subangular (34%), angular (20%), or very angular (3%).

Lithology was determined for clasts in each of the channels. In Channels 1-5, the greatest percentage of clasts are Sappington calcareous siltstone and sandstone and Three Forks silty and brecciated limestone (44%). The remainder of the clasts are Lodgepole limestone (40%), and Jefferson dolomite, limestone, and dolomitic siltstone (16%). Although clasts from the Jefferson Formation constitute only a small portion of clasts in Channels 1-5, the percentage of Jefferson clasts increases from northeast to southwest, from less than 1% in Channel 1, to 26% in Channel 5. Channel 6 has 100% dolomite, limestone, and dolomitic siltstone clasts because its source area lies entirely within the Jefferson Formation.

Interpretation. Clast size in the Sacajawea cirque deposits, for clasts larger than 64 mm, is predominately boulder- and cobble-size, except for terminal lobes which have cobble-size clasts. The presence of the smallest clasts in terminal lobes may result from larger clasts being deposited within in-channel lobes, lateral lobes, and levees. As large clasts are left behind, a thinner more fluid flow proceeds to the terminus and forms a finer terminal lobe.

The large percentage of silt (54%) and clay (10%) in a sample of the matrix suggest that the Three Forks and Sappington shale and siltstone and the lower shale unit of the Lodgepole Formation contribute to the finer matrix. Shale and siltstone are fine grained sedimentary rocks that are less chemically and mechanically resistant in an arid climate than are carbonate rocks such as limestone and dolomite. This is because shale and siltstone contain clay minerals and feldspars which are readily weathered (Garrels and Mackenzie, 1971, p. 145).

Roundness of clasts in the Sacajawea deposits is primarily dependent on source rock and weathering. Distance of transport is short and would not affect roundness. As a majority of the clasts are Sappington calcareous siltstone and sandstone and Three Forks silty and brecciated limestone, the subrounded nature of these clasts suggest

that these units have been extensively affected by chemical weathering.

Lithology was also studied to determine if the talus slopes adjacent to the debris-flow fan contributed clasts to the debris flows. Although none of the debris flows originate in the Lodgepole limestone, forty percent of clasts in the debris-flow deposits are from the Lodgepole limestone, the source rock of the talus slopes. Thus, the talus slopes are contributing clasts to the main gully where debris flows are initiated.

Grading

Description. In the vertical sections exposed on the fan, grading is absent except at the top of the section, where the deposits are inversely graded (Figure 15). Boulders are concentrated at the top of the section, making the deposit coarse-tail inversely graded, while the rest of the deposit is massive with scattered boulders. Also shown in Figure 15 is the clast-supported framework.

Interpretation. The bulk of the Sacajawea cirque deposits are massive, with only the upper portion being coarse-tail inversely graded. The massive bedding is due to the high concentration of clasts deposited rapidly en masse. Eyles and others (1988) state that absence of grading indicates short transport distance from a proximal sediment source. The Sacajawea debris flows were transported only a

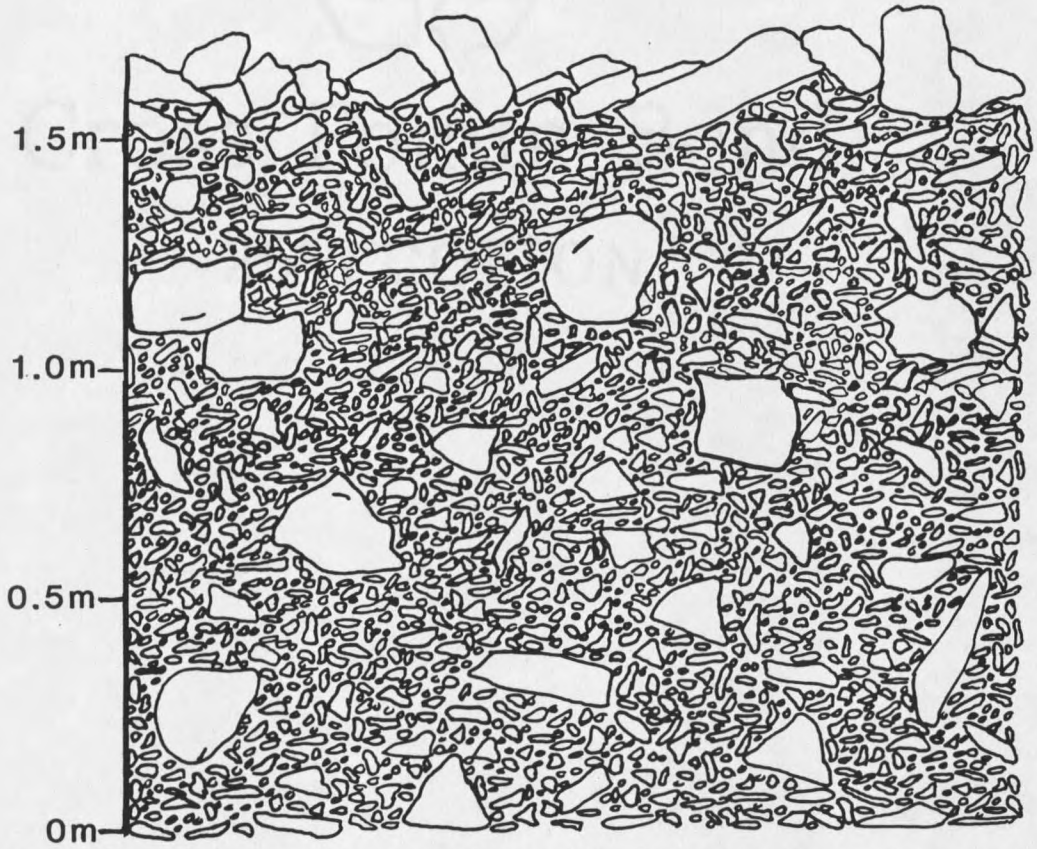

Figure 15. Sketch of exposed vertical section in the main gully showing no grading within the bulk of the deposit and coarse-tail inverse grading at the top of the deposit. Clast-supported framework is also shown.

short distance before being deposited. The top coarse-tail inversely graded portion is due to one or more of the following mechanisms: dispersive pressure, kinetic sieving, or large clasts carried on the top of the flow remaining there after deposition. In poorly sorted sediment, dispersive pressures acting on large colliding particles force them upward into the zone of least shear (Boggs, 1987, p. 62). Kinetic sieving occurs when smaller particles fall through spaces between larger particles during collisions

and displace the larger particles upward. Lastly, coarse-grained material may have fallen from the sides of the channels onto the top of the flow and remained there during transport and subsequent deposition. The dominate process is not known.

TALUS DEPOSITS

Sedimentologic Characteristics

Clast Packing

Description. The deposits on the surface of the talus pile are clast-supported, with cobble- and boulder-size clasts touching. A few pebble-size clasts are present; however, a finer matrix is not found on the surface of the talus pile. The clast-packing at the bottom of the talus pile was not observed in this study, as the talus clasts were too large to remove from the surface of the talus.

Interpretation. Tanner and Hubert (1991) note that the surface of talus deposits are clast-supported. This is because the talus is usually very coarse-grained and finer material falls in between spaces and settles to the bottom of the talus pile.

Clast Fabric

Description. Figure 16 shows the three stereonets produced for the three talus grids. According to the Spheristat program, Grids 1 and 3 show weakly developed girdles and clusters, while Grid 2 shows a moderately developed girdle and cluster. Clast long-axes are oriented

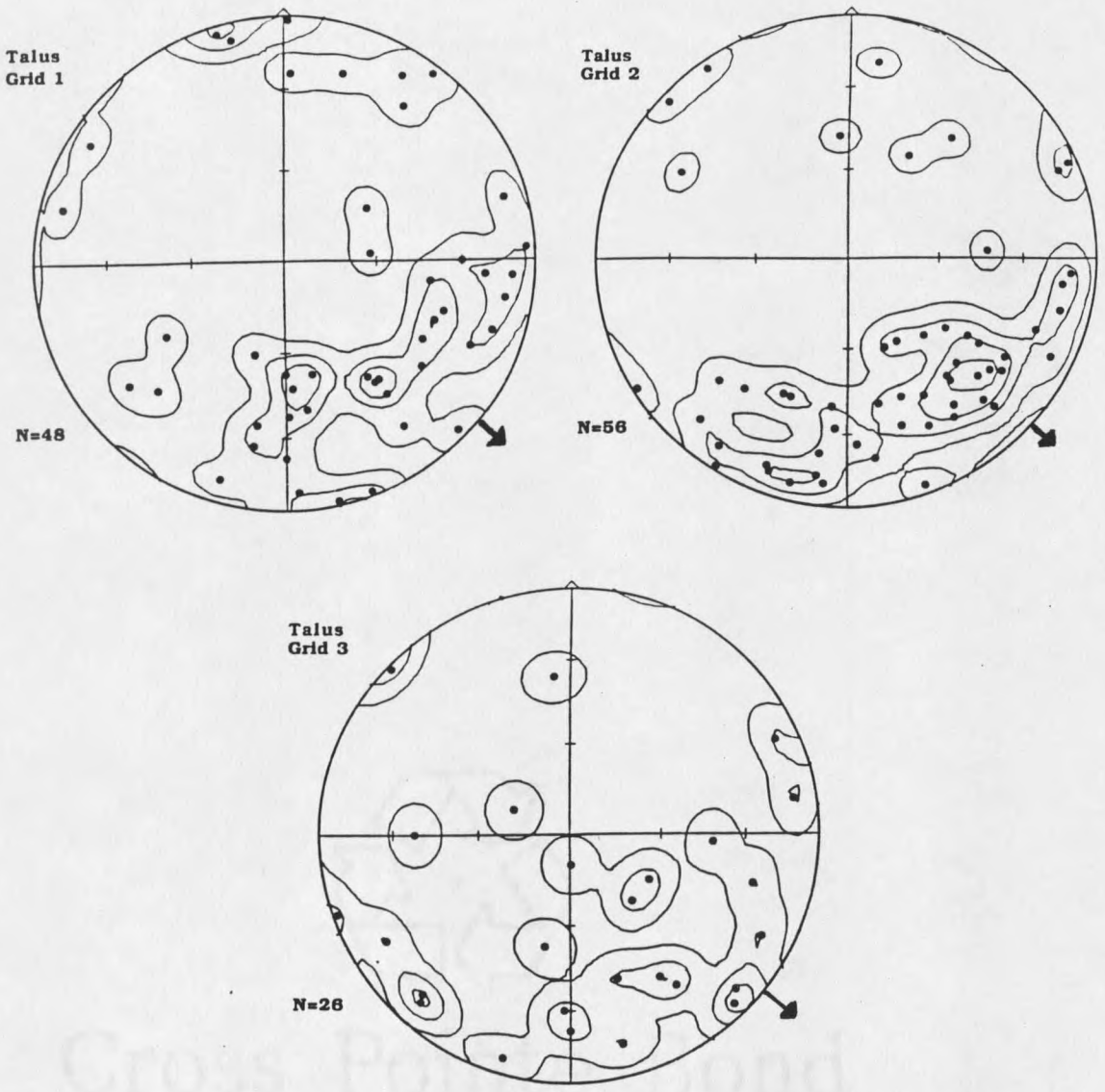

Figure 16. Contoured lower hemisphere Schmidt nets of sampled grids from talus slopes showing orientation of clasts with respect to the downslope direction (given by arrows).

parallel to the slope direction and dip downslope.

Imbrication is more common in platy talus clasts (36%) than in elongate/bladed talus clasts (< 1%). Dip angles in platy clasts range from 2 to 79 degrees (Appendix B).

Two of the three talus stereonets (Grids 2 and 3) display orthorhombic symmetry; however, all three were analyzed by the eigenvalue method (Table 9). This is because for all three talus stereonets, the V_1 azimuths are within 30 degrees of a direction parallel to the slope direction and dip downslope. The S_1 and S_3 values are significant at the 0.05 level for Grids 1 and 2 but not for Grid 3 (Table 9). All the S_1 mean strength values are weak (S_1<0.60). Figure 17 is an eigenvalue ratio graph showing the shape and strength of the talus fabric. All three grids are near the origin of the graph, where weaker fabrics are found (Mills, 1991).

Table 9. Summary of eigenvalue analysis of clast fabric for Sacajawea talus.

Sample	n	Slope Dir.	V_1 Azi.	V_1 Dip	S_1	S_3
Grid 1	48	130	149	30	**0.55**	**0.13**
Grid 2*	56	130	155	30	**0.60**	**0.10**
Grid 3*	26	130	149	33	0.49	0.17

* Orthorhombic samples
Note: Values for slope direction, V_1 azimuth, and V_1 dip are in degrees. Bold S_1 and S_3 values = significant at p<0.05.

Both the A_{0-90} and A_{0-180} values determined for the talus deposit are 21 degrees with a standard deviation of 5 degrees, indicating parallel orientation and downslope dips. The D_1 value of the talus is 31 degrees.

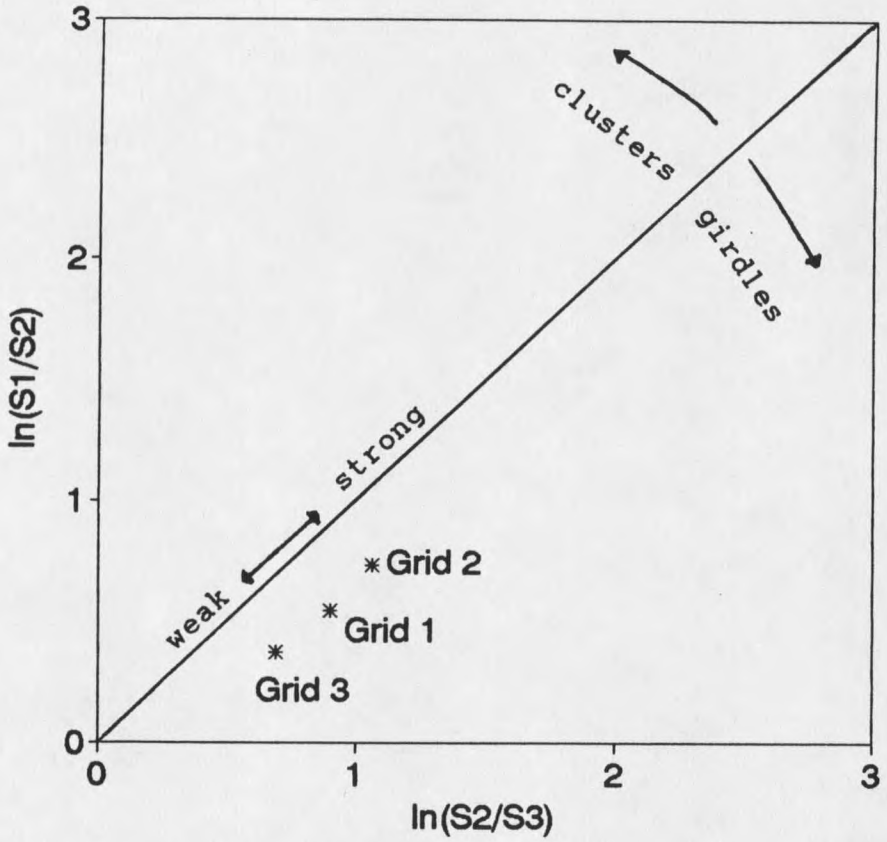

Figure 17. Eigenvalue ratio graph of normalized eigenvalues and their relationship to shape and strength of the talus fabric. Strength increases away from the origin of the diagram. Clusters fall above the center line, girdles below it. Grids 1, 2, and 3 represent the three sample sites or grids where orientation data was collected from the talus slopes. After Woodcock and Naylor (1983).

Interpretation. The characteristics of the Sacajawea talus fabric are similar to other talus fabrics. For example, talus fabrics noted in other studies (McSavaney, in Mills, 1991; Albjar *et al.*, in Mills, 1991; Mills, 1991) also show predominately girdle type distributions, weak fabric strength, and steep dips.

Platy clasts in the talus deposits show some imbrication, as do a few of the elongate/bladed clasts. According to Rapp and Fairbridge (1968), talus clasts of both shapes are often steeply imbricated.

Eigenvalue analysis reveals parallel orientation of clasts, which is commonly cited for modern talus slopes (Tanner and Hubert, 1991). The mean S_1 value of the Sacajawea talus (0.55) is similar to talus in Colorado (S_1=0.56) (McSaveney, in Mills, 1991), as well as talus from both arid and periglacial climates combined (S_1=0.55) (Albjar et al., in Mills, 1991). This result suggests that fabric of talus deposits is weak.

The parallel orientation indicated by the A_{0-90} value of the Sacajawea talus (21 degrees) is similar to other A_{0-90} values: for Colorado talus (38±24 degrees) (McSaveney, in Mills, 1991) and for arid and periglacial talus combined (20 ±11 degrees) (Albjar et al., in Mills, 1991). However, the other studies show high standard deviations, suggesting that there is variability of clast orientation and/or inclusion of non-orthorhombic stereonets. Thus, as for the debris-flow deposits, the A_{0-90} and A_{0-180} values are not as useful as S_1 and S_3 values for comparing talus studies.

The A_{0-180} value of the Sacajawea talus suggests a downslope dip of parallel clasts and this has been confirmed by other studies (McSaveney, in Mills, 1991; Albjar et al., in Mills, 1991). As mentioned previously, dips are steep

for talus in general, and are also steep for this study. The mean value of 31 degrees suggests a strong control on the dip by the slope angle, which ranges from 30 to 34 degrees on the slopes where grids were set up. Mills (1991) also found that study sites located on steep slopes were characterized by steeply dipping clasts.

Clast Size, Roundness, and Lithology

Description. The mean size of clasts larger than 64 mm on the talus surface is 274 mm with a standard deviation of 59 mm, or cobble- to boulder-size. The greatest percentage of talus clasts are subangular (56%). The remainder of the clasts are angular (21%), subrounded (15%), and very angular (8%). By visual inspection, the lithology of the talus deposits is dominately Lodgepole limestone, with a minor amount of Mission Canyon limestone.

Interpretation. The cobble- to boulder-size clasts present on the surface of the talus deposit are the most common clast size for talus surfaces (Tanner and Hubert, 1991). The angular shape of the clasts is due to the short transport distance of the clasts from the outcrop to the talus slope below and lack of weathering of the clasts. The Lodgepole and Mission Canyon limestone clasts did not weather as easily as the subrounded Sappington and Three Forks clasts from the debris-flow deposits. This is because the Lodgepole and Mission Canyon limestone is dense,

carbonate rock which is more resistant to weathering than the more porous calcareous siltstone and silty limestone of the Sappington and Three Forks Formations.

DISCUSSION

Geomorphic Characteristics

This study of the Sacajawea cirque fan and the debris-flow deposits on the fan has documented some important geomorphic characteristics. First, the area of the fan and drainage area are smaller than other documented debris-flow fans, and the small, steep drainage produced a debris-flow dominated rather than a fluvially-dominated fan. The more easily weathered and eroded rock units in the cirque determine the location of the drainage area and whether debris flows or talus will occur. This study also shows that a small drainage area can produce well-formed debris-flow deposits in which continuous levees as well as three types of debris-flow lobes are clearly recognizable. The well-formed levees and lobes provided excellent exposures in which to study and document the sedimentologic characteristics of these debris-flow deposits.

Sedimentologic Characteristics

The study of the sedimentologic characteristics of the Sacajawea cirque debris-flow deposits has contributed to the range of fabrics and sedimentary structures that characterize debris-flow deposits. Deposits have a clast

fabric framework and sedimentary structures that are not cited as common characteristics for debris-flow deposits. The Sacajawea cirque deposits are clast-supported and display massive bedding. Inverse grading is present only at the top of the deposit. These are characteristics also found in hyperconcentrated-flow deposits and stream-flow deposits of the lithofacies Gm from the code system developed by Miall (1978). This study shows that debris-flow deposits can often look very similar to both hyperconcentrated-flow and stream-flow deposits and sedimentologists should use greater caution in interpretation of ancient deposits.

Clast-supported fabric has been cited by many authors (Sharp and Nobles, 1953; Curry, 1966; Lowe, 1979b; Shultz, 1984; Mills, 1984; Tanner and Hubert, 1991), though never recognized as common a characteristic, as has matrix-supported fabric (Innes, 1983; Costa, 1984; Smith, 1986). This study reinforces the view that either clast- or matrix-supported fabrics can develop in debris flows and that clast-supported fabric should also be recognized as a common debris-flow characteristic.

The sedimentologic characteristics of debris-flow deposits provide insight into rheologic or flow characteristics. Using both clast fabric framework and presence or absence of sedimentary structures, Shultz (1984) described four debris-flow regimes representing the entire

flow spectrum, from flows with high yield strength, laminar flow and viscous clast interactions to flows with low yield strength, turbulent flow, and collisional clast interactions. The Sacajawea cirque debris-flow deposits do not fit into any flow type that Shultz (1984) described. Rather, they share attributes of two flow types: Clast-rich debris flows and psuedoplastic debris flows.

Clast-rich debris flows are characterized by deposits that are clast-supported and inversely graded. The flows have a high concentration of clasts and only a few percent clay. Clasts are supported by collisional clast interactions and buoyancy rather than the cohesion of the clayey slurry (Shultz, 1984). As a result, dispersive pressure is increased, producing inverse grading. Laminar flow and high yield strength predominate, producing slow, viscous flows. However, clast-rich debris flows do not leave massive deposits, whereas psuedoplastic debris flows do.

Psuedoplastic debris flows have a low yield strength due to the high water content. Laminar flow is dominant, but turbulence may occur during high-velocity stages and aid in suspending the largest clasts. Matrix strength supports only the smallest clasts, and as a result, dispersive pressure is diminished and coarse flows produce ungraded deposits (Shultz, 1984). The flow characteristics of the Sacajawea cirque debris-flow deposits varied rheologically,

producing the clast-supported, massive to inversely graded deposits.

Many recent debris flow studies use the eigenvalue method to differentiate debris flows from other diamictons (Mills, 1984, 1991; Rappol, 1985; Major and Voight, 1986). This study shows that diamictons are better distinguished by fabric strength than fabric pattern. Future comparative studies using the eigenvalue method should only use orthorhombic samples and fabric strength as an indicator.

Talus Deposits

Overall, the Sacajawea cirque debris-flow and talus deposits are similar sedimentologically because talus deposits contribute clasts to the main gully. These materials are then deposited on the fan as debris flows. About 40 percent of clasts in the debris flows are Lodgepole limestone, the dominant lithology of the talus slopes. Talus clasts are generally cobble-size and larger, resulting in the dominance of large clasts in the debris-flow deposits. This comparison of modern deposits of debris flows and talus has shown that caution should be used in identification of talus deposits in the rock record, as they may appear similar to clast-supported, massive to inversely graded debris-flow deposits.

This study shows that the lithology of rock units which are the source for the debris flows is different than that

for talus slopes. The talus slopes develop from the Lodgepole and Mission Canyon Formations (the Madison Group). The Madison Group is massive and forms the crest of the Bridger Range (Locke and Lageson, 1989). This stratigraphic unit is relatively resistant to chemical and physical weathering and hence to gully formation. The more easily weathered and erodible Three Forks and Sappington shales and calcareous siltstones produce debris flows. These rock types are less resistant to erosion than the Madison Group, their steep dip corresponds to the slope of the land surface, and they are heavily jointed. These factors favor gully formation in the Three Forks and Sappington Formations. Thus, the juxtaposition of rock units of varying relative erodibility produced debris-flow deposits next to talus deposits in Sacajawea cirque.

CONCLUSION

The debris-flow fan in Sacajawea cirque is steep and small (0.03 km^2) with a very small drainage area (0.006 km^2). The deposits found on the fan are thin and have coarse levees bordering channels with well-formed terminal lobes, lateral lobes, and in-channel lobes both inside and outside of the channels. These well-formed deposits can be initiated in narrow, steep gullies or on smooth, steep hillslopes covered with unconsolidated clasts. Between leveed channels are overlapping deposits, weathered lobate forms, and lobate deposits: partially buried accumulations of overbank debris-flow lobes.

The six channels on the fan have both U- and V- shape cross-sectional profiles and are shorter than channel lengths cited in the literature. As the main gully does not connect with any one channel, the channel future flows take appears random. Profiles of the channels show that in-channel lobes block some reaches of the channels, contributing to channel avulsion and to the pattern of deposition on the fan.

Study of debris-flow fabrics reveals clast-supported rather than matrix-supported fabric. This observation suggests that clast-support should be recognized as a common characteristic of debris flows. Qualitative comparison of

debris-flow fabric diagrams shows similarities in scatter of data points, weak fabric, and dominance of parallel orientation with differences in dip angle and orientation of clasts in levees and lobes.

Quantitative analysis of clast fabric by the eigenvalue method shows that clasts in levees have a weak downstream orientation and also dip downstream. This is due to laminar flow. Lobes, on the other hand, show no preferred orientation, due to turbulent flow or reworking of the clasts by running water or post-depositional settling processes such as solifluction. This study finds no relation between clast packing and clast orientation. Debris flows can be distinguished from other diamictons by clast orientation studies.

The textures of the Sacajawea cirque debris-flow deposits are cobble- and boulder-sizes for clasts larger than 64 mm. Forty percent of these size clasts come from the Lodgepole limestone and thus the talus slopes are contributing clasts to the main gully. The large percentages of silt (54%) and clay (10%) in the matrix show that the Three Forks and Sappington shale and siltstone and the shale unit in the Lodgepole contributed the finer matrix because these units are less resistant to weathering. The subrounded nature of cobble- and boulder-size clasts from these units also suggests they have been weathered extensively.

Sedimentary structures are absent in lower portions of the deposits. The deposits are massive due to deposition en masse and to the short transport distance of the flows. However, the tops of the flows are coarse-tail inversely graded due to one or more of the following processes: dispersive pressure, kinetic sieving, or large clasts carried on the top of the flow remaining there after deposition.

The clast fabric of the talus deposits is characterized sedimentologically by a clast-supported framework and clast fabric aligned parallel to the slope direction and dipping downslope at steep angles. Eigenvalue analysis reveals that fabric is weak overall for the talus. Textural analysis reveals that the talus deposit consists of angular, cobble- to boulder-size clasts of Lodgepole limestone.

Overall, the debris-flow and talus deposits do not differ significantly. Both deposits are clast-supported, have weak fabric with clast long-axes oriented parallel to flow or the slope direction, and possess similar clast-sizes.

REFERENCES CITED

Albjar, G., Rehn, J., and Stromquist, L., 1979, Notes on talus formation in different climates: Geografiska Annaler, v. 61A, p. 179-185.

Blair, T. C., 1987, Sedimentary processes, vertical stratification sequences, and geomorphology of the Roaring River alluvial fan, Rocky Mountain National Park, Colorado: Journal of Sedimentary Petrology, v. 57, p. 1-18.

Blair, T. C., and McPherson, J. G., 1992, The Trollheim alluvial fan and facies model revisited: Geological Society of America Bulletin, v. 104, p. 762-769.

Boggs, S. Jr., 1987, Principles of sedimentology and stratigraphy: Columbus, OH, Merrill, 784 p.

Boulton, G. S., 1971, Till genesis and fabric in Svalbord, Spitsbergen, in R. P. Goldwaite, ed., Till-a Symposium: Columbus, Ohio State University Press, p. 41-72.

Broscoe, A. J., and Thomson, S., 1969, Observations on an alpine mudflow, Steel Creek, Yukon: Canadian Journal of Earth Sciences, v. 6, p. 219-229.

Costa, J. E., 1984, Physical geomorphology of debris flows, in Costa, J. E., and Fleisher, P. J., eds., Developments and Applications of Geomorphology: Berlin, Springer-Verlag, p. 268-317.

_____ 1988, Rheologic, geomorphic, and sedimentologic differentiation of water floods, hyperconcentrated flows, and debris flows: in V. R. Baker, R. C. Kochel, and P. C. Patton, eds., Flood Geomorphology, Wiley, New York, p. 113-122.

Curry, R. R., 1966, Observation of alpine mudflows in the Tenmile Range, Central Colorado: Geological Society of America Bulletin, v. 77, p. 771-776.

Desloges, J. R., and Gardner, J. S., 1984, Process and discharge estimation in ephemeral channels, Canadian Rocky Mountains: Canadian Journal of Earth Sciences, v. 21, p. 1050-1060.

Enos, P., 1977, Flow regimes in debris flows: Sedimentology, v. 24, p. 133-142.

Eyles, N., Eyles, C.H., and McCabe, A.M., 1988, Late Pleistocene subaerial debris-flow facies of the Bow Valley, near Banff, Canadian Rocky Mountains: Sedimentology, v. 35, p. 465-480.

Eyles, N., and Kocsis, S., 1988, Sedimentology and clast fabric of subaerial debris flow facies in a glacially-influenced alluvial fan: Sedimentary Geology, v. 59, p. 15-28.

Filipov, A. J., 1986, Sedimentology of debris-flow deposits, west flank of the White Mountains, California: Master's Thesis, University of Massachusetts, 197 p.

Fryxell, F. M. and Horberg, L., 1943, Alpine mudflows in Grand Teton National Park, Wyoming: Geological Society of America Bulletin, v. 54, 457-472.

Garrels, R. M., and Mackenzie, F. T., Evolution of sedimentary rocks: N. W. Norton & Co., Boston, MA, 397p.

Hampton, M. A., 1975, Competence of fine-grained debris flows: Journal of Sedimentary Petrology, v. 45, p. 834-844.

Harvey, A. M., 1992, Controls on sedimentary style on alluvial fans: in D. Billi, R. D. Hey, C. R. Thorne, and P. Tacconi, eds., Dynamics of Gravel-bed Rivers, John Wiley and Sons, New York, NY., p. 519-535.

Hubert, J. F., and Filipov, A. J., 1989, Debris-flow deposits in alluvial fans on the west flank of the White Mountains, Owens Valley, California, U.S.A.: Sedimentary Geology, V. 61, P. 177-205.

Innes, J. L., 1983, Debris flows: Progress in Physical Geography, v. 7, p. 469-501.

Johnson, A. M., and Rodine, J. R., 1984, Debris flow, in D. Brunsden and D. B. Prior, eds., Slope Instability: John Wiley and Sons, New York, NY.,p. 263-277.

Kochel, R. C., 1990, Humid fans of the Appalachian Mountains: *in* A. H., Rachocki, and M. Church, eds., Alluvial Fans, John Wiley & Sons, New York, NY., p. 109-128.

Lageson, D. R., 1989, Reactivation of a Proterozoic continental margin, Bridger Range, Southwestern Montana: *in* D.E. French and R. F. Grabb, eds., 1989 Field Conference Guidebook: Montana Centennial Edition. Montana Geological Society, v. 1, p. 279-298.

Lawson, D. E., 1979a, A comparison of the pebble orientations in ice and deposits of the Matanuska Glacier, AK: Journal of Geology, v. 84, p. 629-645.

Lindholm, R., 1987, A practical approach to sedimentology: Allen & Unwin, London, 276 p.

Lindsay, J. F., 1968, The development of clast fabric in mudflows: Journal of Sedimentary Petrology, v. 38, p. 1242-1253.

Locke, W. W., and Lageson, D. R., 1989, Trip 4 road log: Geology and geomorphology of the Rocky Mountains/Great Plains transition: *in* D. E. French and R. L. Grabb, eds., 1989 Field Conference Guidebook: Montana Centennial Edition. Montana Geological Society, v. 1, p. 462-476.

Lowe, D. R., 1982, Sediment gravity flows: II. Depositional models with special reference to the deposits of high-density turbidity currents: Journal of Sedimentary Petrology, v. 52, p. 279-297.

Major, J. J., and Voight, B., 1986, Sedimentology and clast orientations of the 18 May 1980 Southwest-flank lahars, Mount St. Helens, Washington: Journal of Sedimentary Petrology, v. 56, p. 691-705.

Mark, D. M., 1973, Analysis of axial orientation data, including till fabrics: Geological Society of America Bulletin, v. 84, p. 1369-1374.

_____ 1974, On the interpretation of till fabrics: Geology, v. 2, p. 101-104.

McMannis, W. J., 1955, Geology of the Bridger Range, Montana: Geological Society of America Bulletin, v. 66, p. 1385-1430.

McSaveney, E. R., 1979, The surficial fabric of rockfall talus: *in* M. Morisawa, ed., Quantitative geomorphology: some aspects and applications, Proceedings of the second annual geomorphology symposium series held at Binghamton, N.Y., October 15-16, 1971: State University of NY Publications in Geomorphology, p. 181-197.

Miall, A. D., 1978, Lithofacies types and vertical profile models in braided river deposits: a summary: in A. D. Miall, ed., Fluvial Sedimentology, Canadian Society of Petroleum Geologists Memoir 5, p. 605-625.

Mills, H. H., 1984, Clast orientation in Mount St. Helens debris-flow deposits, North fork Toutle River, Washington: Journal of Sedimentary Petrology, v. 54. p. 626-634.

_____ 1991, Three-dimensional clast orientation in glacial and mass-movement sediments-a compilation and preliminary analysis: U.S. Geological Survey Open File Report 90-128, 71 p.

Nelson, F. E., 1985, A preliminary investigation of solifluction macrofabrics: Catena, v. 12, p. 23-33.

Nyberg, R., unpublished, Measurements from debris flows in Sweden, in H. H. Mills, 1991, Three dimensional clast orientation in glacial and mass-movement sediments-a compilation and preliminary analysis: U.S. Geological Survey Open File Report 90-128, 71 p.

Ono, Y., 1990, Alluvial fans in Japan and South Korea: in Rachocki, A. H., and Church, M., eds., Alluvial fans: A field approach: John Wiley & Sons, p. 91-106.

Owens, I F., 1973, Alpine mudflows in the Nigel Pass Area, Canadian Rocky Mountains: Master's thesis, University of Toronto, 182 p.

Pierson, T. C., and Costa, J. E., 1987, A rheologic classification of subaerial sediment-water flows, in Costa, J. E., and Wieczorek, G. F., eds., Debris flows/avalanches: process, recognition, and mitigation; Reviews in Engineering Geology, v. 7: Boulder, CO., Geological Society of America, p. 1-12.

Rapp, A., and Fairbridge, R. W., 1968, Talus fan or cone; scree and cliff debris: in R. W. Fairbridge, eds., The Encyclopedia of Geomorphology. Dowden , Hutchinson & Ross, p. 1106-1109.

Rapp, A., and Nyberg, R., 1981, Alpine debris flows in northern Scandinavia: Geografiska Annaler, v. 63A, p. 183-196.

Rappol, M., 1985, Clast fabric strength in tills and debris flows compared for different environment: Geologie en Mijnbouw, v. 64, p. 327-332.

_____ 1986, Aspects of ice flow patterns, glacial sediments, and stratigraphy in northwest New Brunswick, in Current Research, part B: Geological Survey of Canada Paper 86-1B, p. 233-237.

Robin, P. F., and Jowett, E. C., 1986, Computerized density contouring and statistical evaluation of orientation data using counting circles and continuous weighting functions: Tectonophysics, v. 121, p. 207-223.

Rodine, J. D., and Johnson, A. M., 1976, The ability of debris, heavily freighted with coarse clastic materials, to flow on gentle slopes: Sedimentology, v. 23, p. 213-234.

Ross, R. L., and Hunter, H. E., 1976, Climax vegetation of Montana-based on soils and climate: Soil Conservation Service, Bozeman, MT., 64 p.

Sharp, R. P., 1942, Mudflow levees: Journal of Geomorphology, v. 5, p. 222-227.

Sharp, R. P., and Nobles, L. H., 1963, Mudflow of 1941 at Wrightwood, Southern California: Geological Society of America Bulletin, v. 64, p. 547-560.

Schmitt, J. G., MSU, personal communication, 1/10/92.

Shultz, A. W., 1984, Subaerial debris-flow deposition in the upper Paleozoic Cultler Formation, western Colorado: Journal of Sedimentary Petrology, v. 54, p. 759-772.

Smith, G. A., 1986, Coarse-grained nonmarine volcaniclastic sediment: Terminology and depositional process: Geological Society of America Bulletin, v. 97, p. 1-10.

Takahashi, T., 1981, Debris flow: Annual Review of Fluid Mechanics, v. 13, p. 57-77.

Tanner, L. H., and Hubert, J. F., 1991, Basalt breccias and conglomerates in the lower Jurassic McCoy Brook Formation, Fundy Basin, Nova Scotia: Differentiation of talus and debris-flow deposits: Journal of Sedimentary Petrology, v. 61-p. 15-27.

Whipple, K. X., and Dunne, T., 1992, The influence of debris-flow rheology on fan morphology, Owens Valley, California: Geological Society of America Bulletin, V. 104, p. 887-900.

White, S. E., 1981, Alpine mass movement forms (noncatastrophic): classification, description, and significance: Arctic and Alpine Research, v. 13, p. 127-137.

Woodcock, N. H., and Naylor, M. A., 1983, Randomness testing in three-dimensional orientation data: Journal of Structural Geology, v. 5, p. 539-548.

APPENDICES

APPENDIX A

TREND AND PLUNGE DATA

Table 10. Trend (T) and plunge (P) data for debris-flow levees.

T	P	T	P	T	P	T	P	T	P
106	55	193	26	227	9	272	20	123	13
46	36	94	22	177	31	116	12	297	5
306	14	212	35	203	38	98	17	314	46
99	36	237	17	229	20	275	42	208	16
49	54	188	13	101	14	132	38	298	16
52	34	6	28	72	16	290	14	291	4
86	48	107	6	70	41	300	6	364	15
87	21	114	49	322	23	104	29	238	8
348	83	96	34	285	52	101	16	45	33
345	3	289	20	297	30	129	52	234	19
252	54	170	16	82	62	284	40	55	6
237	10	294	26	16	36	350	8	249	2
115	36	113	20	367	20	82	52	91	22
74	13	193	17	151	22	322	11	167	26
73	10	70	25	110	26	170	18	356	16
103	13	94	15	76	12	354	14	281	24
151	12	36	51	226	18	203	21	136	16
69	16	159	17	64	36	251	17	156	79
114	10	55	32	137	29	115	32	30	55
44	18	57	40	282	26	276	14	356	20
107	17	118	51	105	15	96	24	174	32
329	54	139	6	203	10	314	20	43	20
76	8	66	48	170	20	240	73	3	2
335	60	136	20	66	30	171	20	229	33
329	28	187	16	200	40	150	46	333	14
330	22	317	14	8	2	102	20	219	2
119	16	114	17	104	4	69	20	2	6
292	12	3	28	109	34	306	2	187	81

Table 10 (continued)

104	28	107	27	180	14	22	15	141	4
209	66	62	30	166	15	70	36	174	2
160	6	110	32	160	6	257	51	44	44
80	20	98	26	173	18	280	12	118	44
188	48	270	26	90	12	150	60	76	24
201	16	227	10	124	52	187	26	72	26
105	34	98	36	73	27	9	27	56	9
129	40	51	53	29	54	5	32	70	37
82	42	308	14	7	19	169	3	124	25
215	8	166	18	355	20	125	19	20	82
166	26	160	58	76	2	306	10	90	34
98	10	5	8	210	12	99	26	120	28
321	4	199	18	73	17	156	6	65	5
97	20	34	38	190	25	138	16	338	14
160	8	152	49	138	20	186	53	308	34
143	8	220	22	35	14	320	15	216	15
232	3	76	16	335	40	163	10	36	29
192	6	108	20	77	21	294	30	107	56
87	21	73	10	286	2	136	20	104	36
140	45	140	45	196	6	132	30	322	7
344	57	148	42	88	18	315	8	341	6
174	13	170	24	38	32	90	2	28	30
53	8	160	39	140	49	98	32	158	16
79	26	300	46	135	16	99	10	154	24
264	8	232	2	73	38	117	11	242	9
268	4	110	26	66	13	165	4	173	4
111	22	101	56	286	3	64	16	286	24
104	13	358	15	313	2	156	16	140	10
179	7	129	4	108	32	119	10	294	14
204	5	192	28	0	37	380	18	178	25

Table 11. Trend (T) and plunge (P) data for debris-flow lobes.

T	P	T	P	T	P	T	P	T	P
5	26	166	46	263	50	239	22	147	31
140	10	256	72	183	22	166	42	165	10
81	6	281	6	260	54	290	14	33	18
264	43	320	8	324	16	130	36	1	37
134	10	245	30	220	20	148	2	200	14
107	18	97	24	231	38	193	53	360	28
40	30	315	34	210	38	180	8	240	59
288	57	91	29	21	36	304	4	330	6
344	24	186	4	112	6	122	28	49	28
257	4	300	22	264	40	296	64	151	2
25	24	145	40	355	8	229	34	151	2
83	18	290	30	270	8	161	10	108	24
288	5	113	33	30	37	234	60	136	28
157	27	293	6	34	4	183	10	210	23
197	26	266	12	293	62	334	40	160	20
85	54	360	12	195	16	62	23	218	19
28	16	190	7	230	5	124	22	352	44
110	6	343	10	338	56	330	72	306	20
205	40	284	32	222	60	31	43	340	58
0	43	20	18	315	60	106	36	215	12
293	40	206	21	139	4	164	14	222	8
96	7	275	5	104	4	246	10	55	16
125	30	169	16	262	15	106	3	140	38
130	6	124	12	96	4	97	18	216	4
287	17	105	17	248	10	179	9	287	3
328	36	46	10	114	42	270	35	245	33
90	44	186	26	324	30	339	57	271	12
220	43	232	64	158	46	51	68	43	16

Table 12. Trend (T) and plunge (P) data for talus slopes.

T	P	T	P	T	P	T	P
190	26	115	20	144	28	182	30
85	62	232	22	158	58	193	52
57	58	135	4	40	36	197	7
37	22	17	21	214	10	178	80
238	44	172	40	94	11	118	14
32	12	90	30	30	50	223	14
344	4	108	34	238	2	105	25
145	20	120	37	188	22	148	33
168	2	87	4	162	30	180	22
180	22	112	36	356	48	270	38
38	4	74	10	172	20	354	36
128	32	197	10	122	26	294	70
94	10	225	29	116	10	240	16
109	14	198	58	150	58	137	60
144	40	98	41	154	26	120	60
142	34	177	8	135	17	313	2
190	40	284	10	368	20	166	14
145	43	143	34	202	40	222	11
177	48	97	14	205	40	251	2
167	52	184	32	111	20	145	27
347	8	134	39	126	50	133	10
1	2	201	12	159	40	136	6
167	52	66	4	136	54	65	10
302	10	126	24	168	40	162	39
179	38	132	30	177	26	93	42
100	12	123	42	188	13	81	10
2	24	140	36	194	8	232	22
160	2	324	4	136	22	135	4
98	41	104	13	200	10	94	21

APPENDIX B

PERCENT IMBRICATED CLASTS

Table 13. Percent of imbricated clasts from debris-flow and talus deposits.

Debris Flows/ Talus	Clast Shape	Type of Deposit	Total # of Clasts Measured	# of Imbri-cated Clasts	% of Imbri-cated Clasts
Debris Flows	Elongate/ Bladed	Levee	326	31	9
		Lateral Lobe	50	9	18
		In-channel Lobe	60	8	13
		Terminal Lobe	45	5	11
		Total	481	53	11
	Platy	Levee	64	16	25
		Lateral Lobe	3	2	67
		In-channel Lobe	8	1	13
		Terminal Lobe	8	2	25
		Total	83	25	25
Talus	Elongate/ Bladed	_____	131	3	1
	Platy	--------	14	5	36

PLATE 1
OBLIQUE PHOTO AND GEOMORPHIC MAP OF THE SACAJAWEA DEBRIS-FLOW FAN: CHANNELS 2-6*

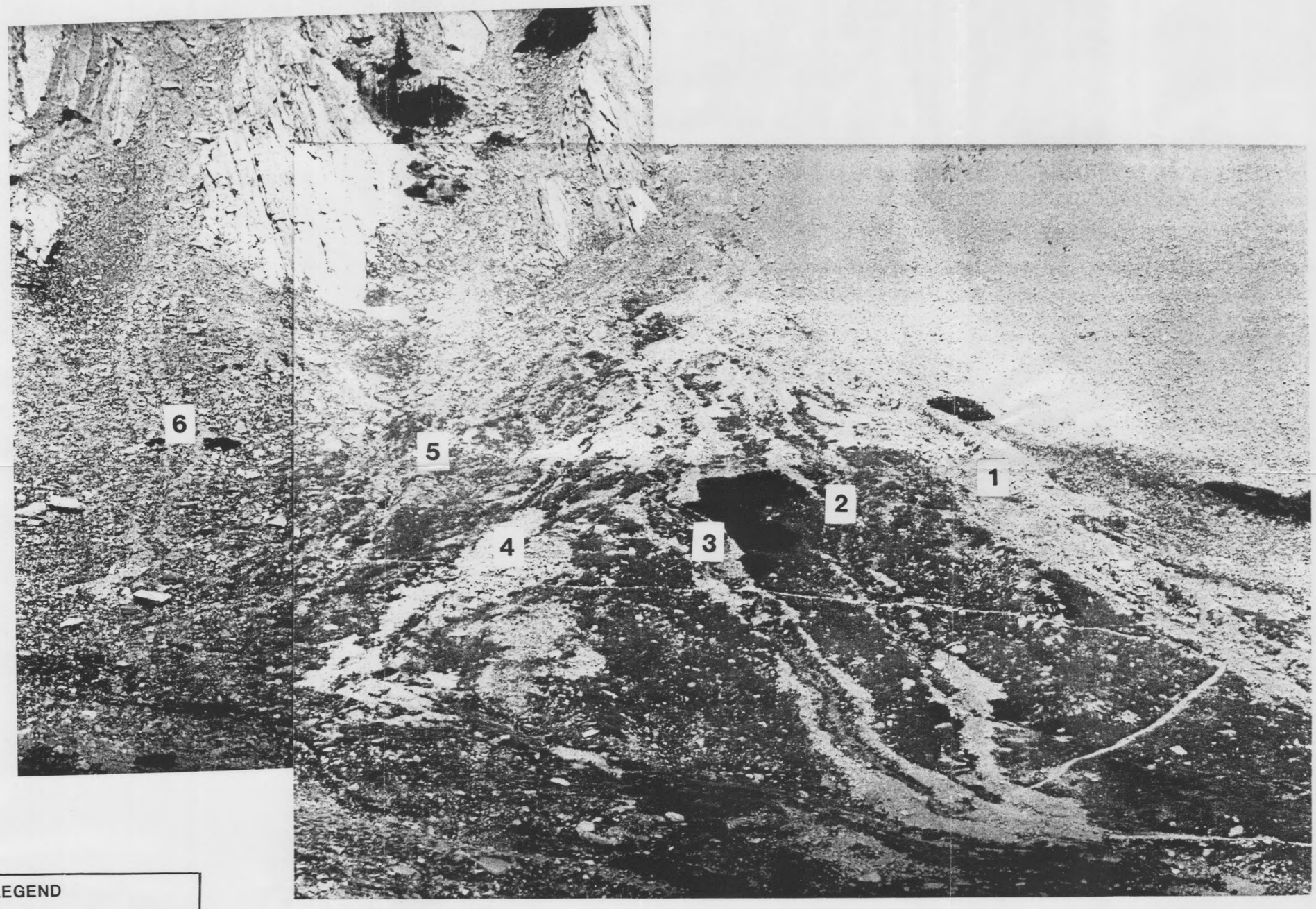

LEGEND

- Well-defined channel
- Channel with boulder levees
- Partially filled channel
- TLB Terminal lobe
- LLB Lateral lobe
- ICLB In-channel lobe
- OD Overlapping deposits
- WLF Weathered lobate forms
- LD Lobate deposits
- Bedrock
  - D_j = Devonian Jefferson
  - D_{tf} Devonian Three Forks
- Sample Sites

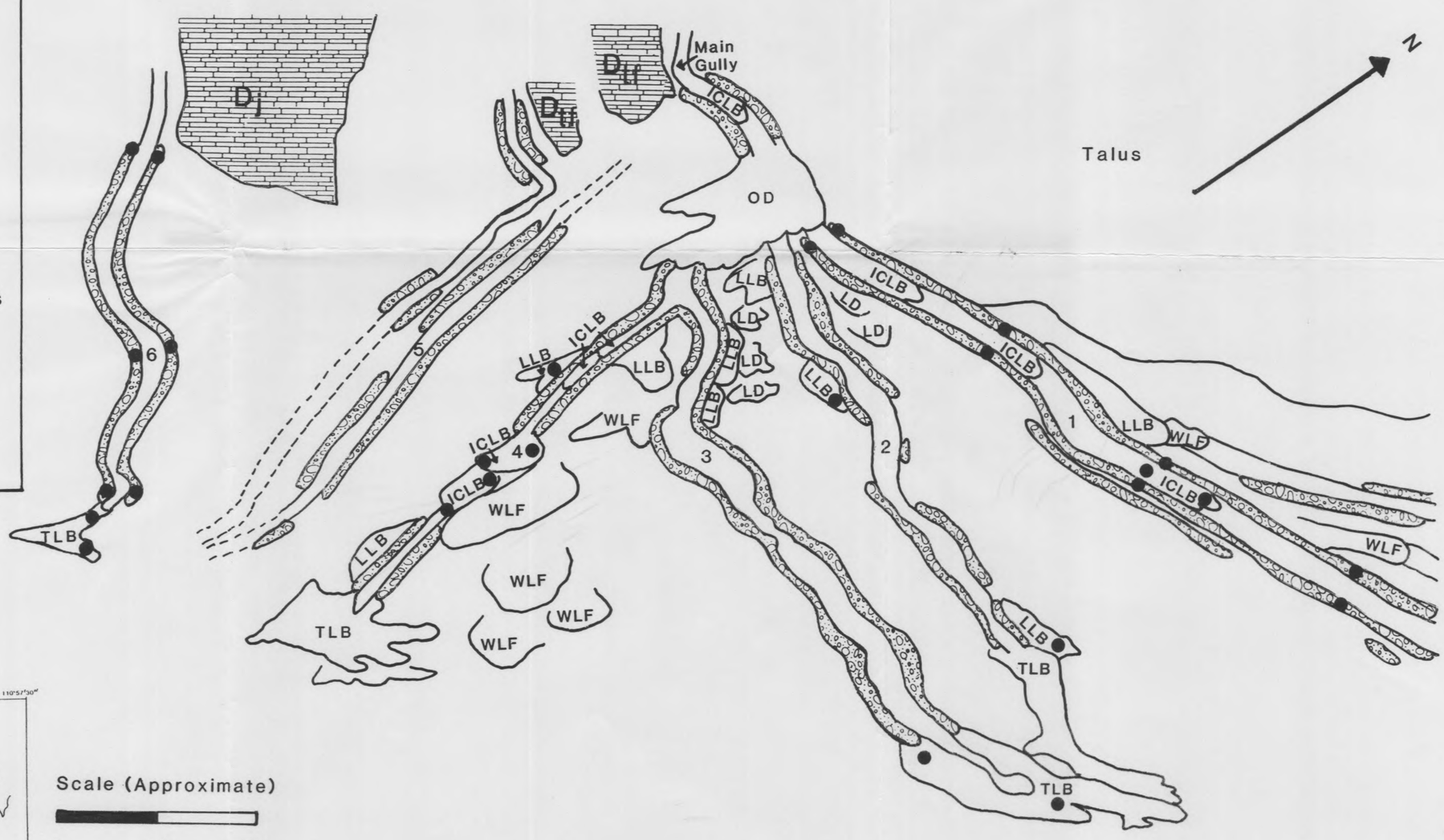

LOCATION MAP

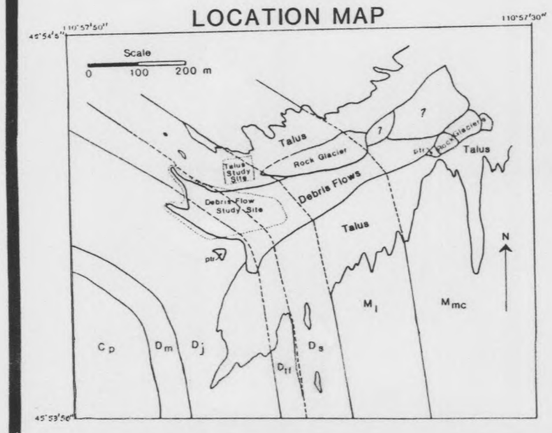

Scale (Approximate)

0 10 20

*Sedimentology of Alpine Debris-Flow and Talus Deposits in Sacajawea Cirque Bridger Range, Montana

by Amanda Vrooman Werner

Master of Science Thesis
Montana State University
Bozeman, Montana
May, 1994

PLATE 2

OBLIQUE PHOTO AND GEOMORPHIC MAP OF THE SACAJAWEA DEBRIS-FLOW FAN: CHANNELS 1-3*

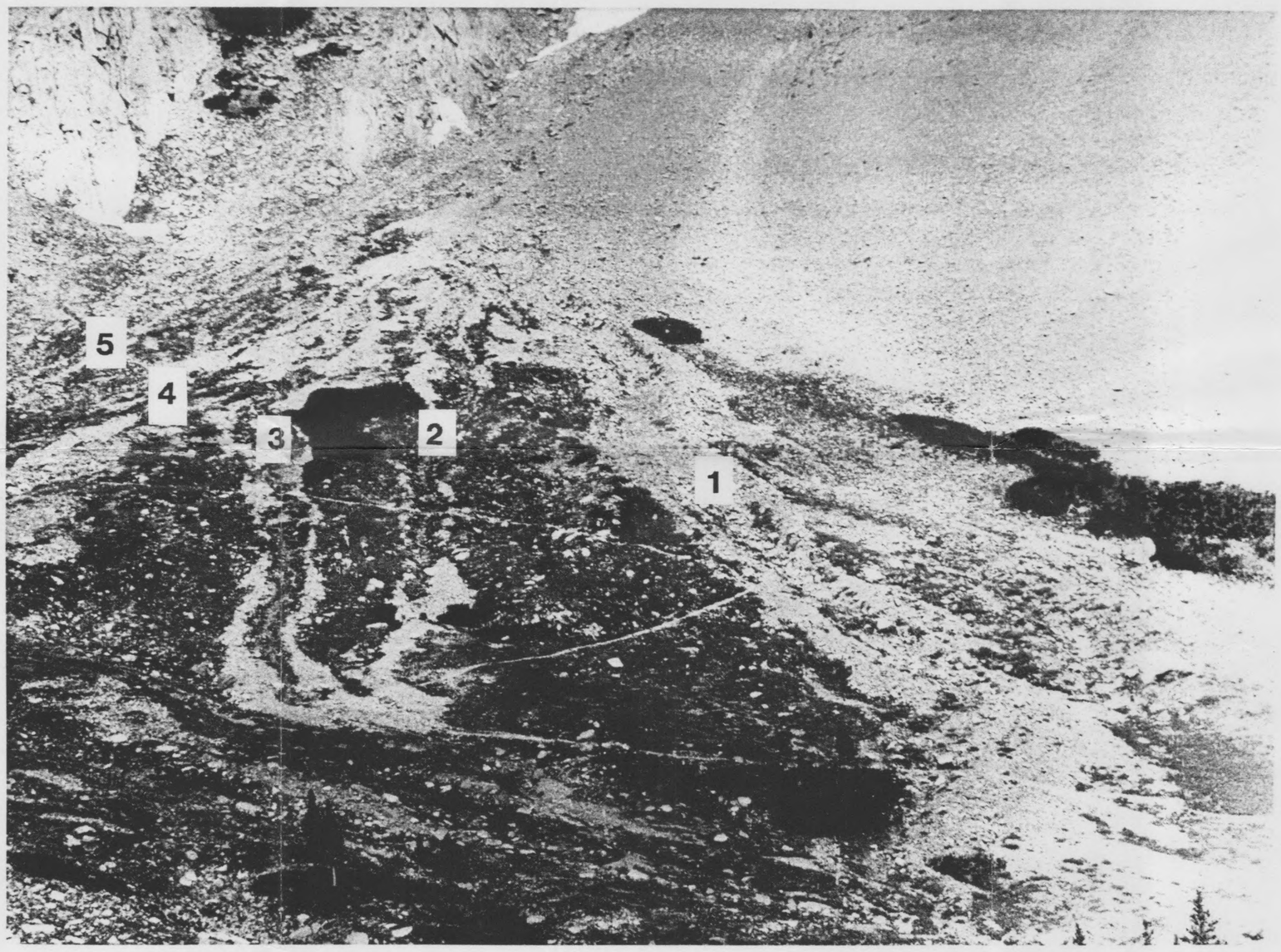

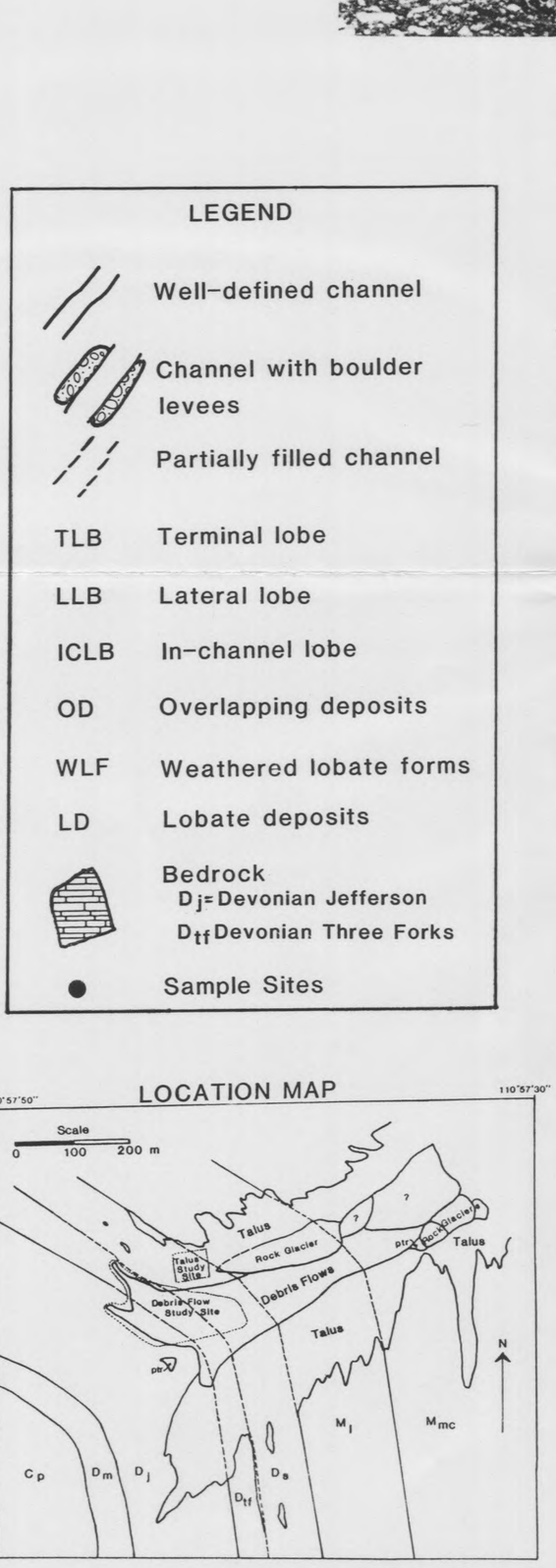

LEGEND

- Well-defined channel
- Channel with boulder levees
- Partially filled channel
- TLB Terminal lobe
- LLB Lateral lobe
- ICLB In-channel lobe
- OD Overlapping deposits
- WLF Weathered lobate forms
- LD Lobate deposits
- Bedrock
  - D_j = Devonian Jefferson
  - D_{tf} Devonian Three Forks
- Sample Sites

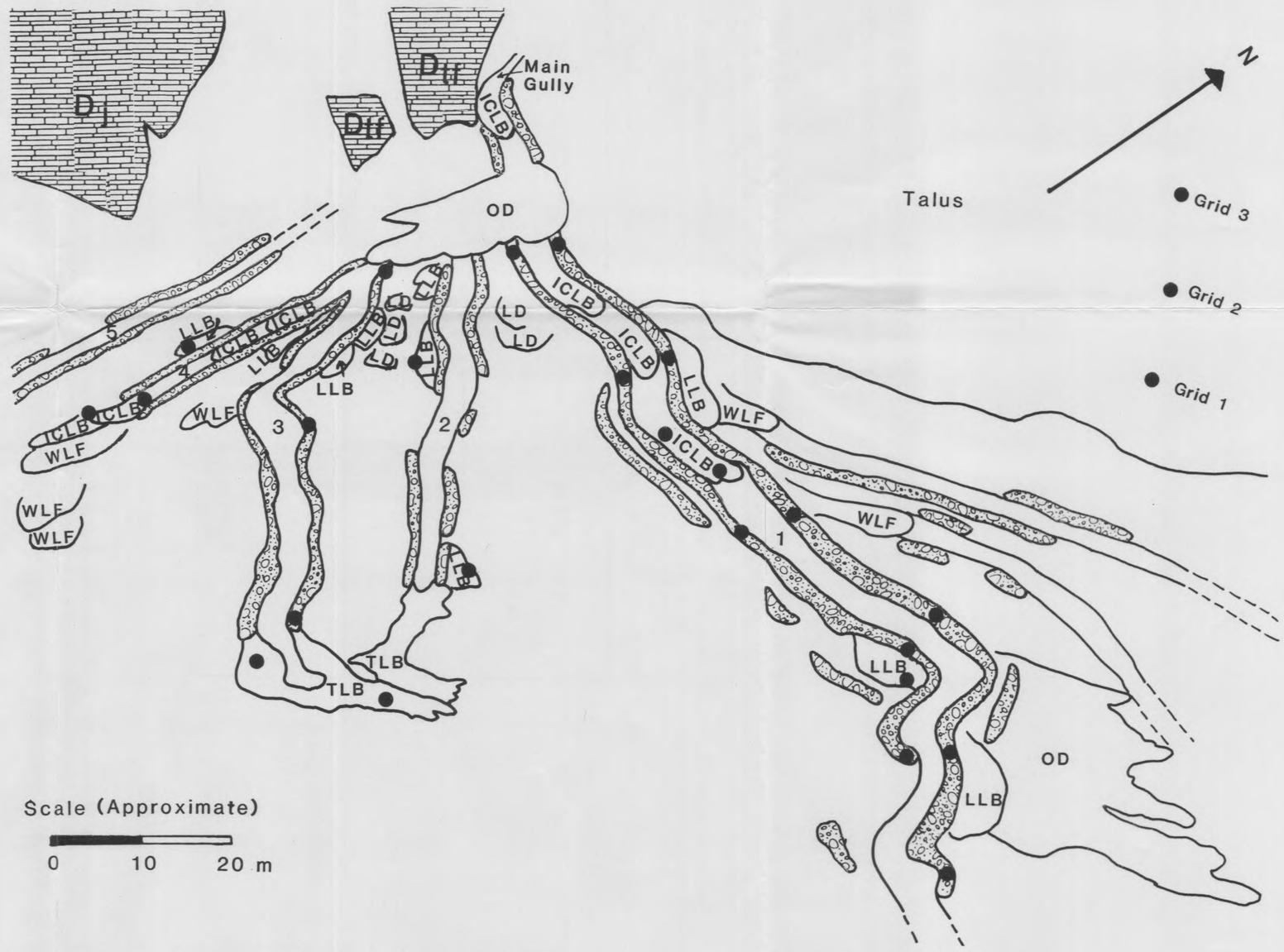

Scale (Approximate)

0 10 20 m

*Sedimentology of Alpine Debris-Flow and Talus Deposits in Sacajawea Cirque Bridger Range, Montana

by Amanda Vrooman Werner

Master of Science Thesis
Montana State University
Bozeman, Montana
May, 1994